

Table 1B-2 Important Functions and their Units at a Receive Volume Aperture

Function	Description	Units
$y_M(t, \mathbf{r}_R)$	output acoustic signal (velocity potential) from the fluid medium, which is also the input acoustic signal to the receive aperture (i.e., it is the acoustic field incident upon the receive aperture) at time t and location $\mathbf{r}_R = (x_R, y_R, z_R)$	m^2/sec
$Y_M(\eta, \mathbf{r}_R)$	complex frequency spectrum of the acoustic field incident upon the receive aperture at location $\mathbf{r}_R = (x_R, y_R, z_R)$	$(\text{m}^2/\text{sec})/\text{Hz}$
$\alpha_R(t, \mathbf{r}_R)$	impulse response of the receive aperture at time t and location $\mathbf{r}_R = (x_R, y_R, z_R)$	$((V/(\text{m}^2/\text{sec}))/\text{m}^3)/\text{sec}$
$A_R(\eta, \mathbf{r}_R)$	complex frequency response of the receive aperture at $\mathbf{r}_R = (x_R, y_R, z_R)$, also known as the complex receive aperture function	$(V/(\text{m}^2/\text{sec}))/\text{m}^3$
$\mathcal{D}_R(\eta, r_s, \beta)$	near-field beam pattern (directivity function) of the receive aperture	$V/(\text{m}^2/\text{sec})$
$D_R(\eta, \beta)$	far-field beam pattern (directivity function) of the receive aperture	$V/(\text{m}^2/\text{sec})$
$y(t, \mathbf{r}_R)$	output electrical signal from the receive aperture at time t and location $\mathbf{r}_R = (x_R, y_R, z_R)$	V/m^3
$Y(\eta, \mathbf{r}_R)$	complex frequency spectrum of the output electrical signal at location $\mathbf{r}_R = (x_R, y_R, z_R)$ of the receive aperture	$(\text{V}/\text{Hz})/\text{m}^3$
$y(t)$	total output electrical signal from the receive aperture	V

Comments

- the units of a scalar velocity potential are m^2/sec

Chapter 2

Complex Aperture Theory – Linear Apertures

2.1 The Far-Field Beam Pattern of a Linear Aperture

Before we begin our discussion, a few comments concerning notation are in order. We shall drop the subscript notation T and R which was used in [Chapter 1](#) to distinguish between transmit and receive apertures, respectively, since we shall now be concerned with apertures in general. Also, the position vectors \mathbf{r}_T and \mathbf{r}_R , which were used to identify the locations of points on the surfaces of transmit and receive apertures, respectively, shall be replaced by the position vector to an aperture point \mathbf{r}_A . And finally, the parameters R_0 and R_R , which were used to designate the maximum radial extent of transmit and receive apertures, respectively, shall be replaced by the maximum radial extent of an aperture R_A . Whenever we need to make a clear distinction between transmit and receive apertures, we shall reintroduce the original subscript notation established in [Chapter 1](#).

In this section we shall demonstrate that the far-field beam pattern of a linear aperture is just a special case of the far-field beam pattern of a volume aperture. In [Section 1.3](#) it was shown that the far-field beam pattern (directivity function) of a closed-surface, volume aperture – based on the Fraunhofer approximation of a time-independent, free-space, Green's function – is given by the following three-dimensional spatial Fourier transform:

$$D(f, \boldsymbol{\alpha}) = F_{\mathbf{r}_A} \{ A(f, \mathbf{r}_A) \} = \int_{-\infty}^{\infty} A(f, \mathbf{r}_A) \exp(+j2\pi\boldsymbol{\alpha} \cdot \mathbf{r}_A) d\mathbf{r}_A, \quad (2.1-1)$$

where

$$\mathbf{r}_A = (x_A, y_A, z_A), \quad (2.1-2)$$

$$\boldsymbol{\alpha} = (f_X, f_Y, f_Z), \quad (2.1-3)$$

$$\boldsymbol{\alpha} \cdot \mathbf{r}_A = f_X x_A + f_Y y_A + f_Z z_A, \quad (2.1-4)$$

$$d\mathbf{r}_A = dx_A dy_A dz_A, \quad (2.1-5)$$

and $F_{\mathbf{r}_A} \{ \cdot \}$ is shorthand notation for $F_{x_A} F_{y_A} F_{z_A} \{ \cdot \}$. The complex aperture function $A(f, \mathbf{r}_A)$ can be expressed as

$$A(f, \mathbf{r}_A) = a(f, \mathbf{r}_A) \exp[+j\theta(f, \mathbf{r}_A)], \quad (2.1-6)$$

where $a(f, \mathbf{r}_A)$ is the *amplitude response* and $\theta(f, \mathbf{r}_A)$ is the *phase response* of the aperture at \mathbf{r}_A . Both $a(f, \mathbf{r}_A)$ and $\theta(f, \mathbf{r}_A)$ are *real* functions. The function $a(f, \mathbf{r}_A)$ is also known as the *amplitude window*. The units of $a(f, \mathbf{r}_A)$ and, hence, $A(f, \mathbf{r}_A)$ depend on whether the aperture is a transmit aperture (see Table 1B-1 in Appendix 1B) or a receive aperture (see Table 1B-2 in Appendix 1B). The units of $\theta(f, \mathbf{r}_A)$ are radians.

Now consider the case of a *linear aperture* of length L meters lying along the X axis as shown in Fig. 2.1-1. A linear aperture can represent either a single electroacoustic transducer (e.g., a continuous line source or receiver) or a linear array of many individual electroacoustic transducers. If a linear aperture represents a single electroacoustic transducer that is being used in the active mode, that is, as a transmitter; then this physical situation corresponds to the classic problem of a continuous line source. Also shown in Fig. 2.1-1 is a field point with spherical coordinates (r, θ, ψ) . The field point is in the far-field region of the aperture, where the range r satisfies the Fraunhofer (far-field) range criterion given by $r > \pi R_A^2 / \lambda > 2.414 R_A$ [see either (1.2-39) or (1.2-93)], and $R_A = L/2$ is the maximum radial extent of the linear aperture.

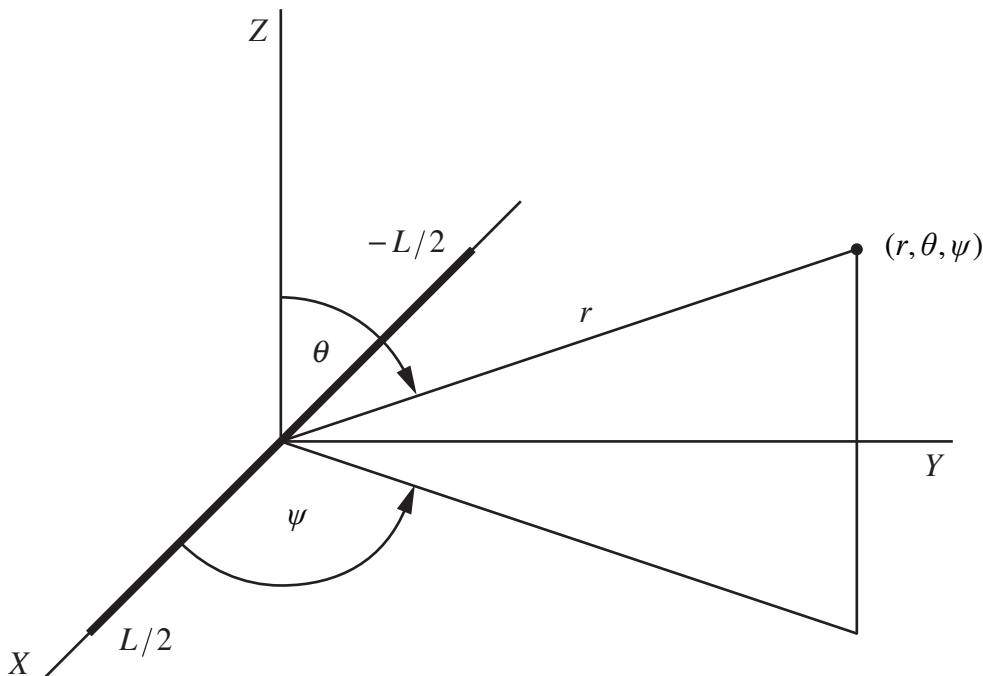


Figure 2.1-1 Linear aperture of length L meters lying along the X axis. Also shown is a field point with spherical coordinates (r, θ, ψ) .

Since the linear aperture in Fig. 2.1-1 is lying along the X axis, the position vector to a point on the surface of the aperture is given by

$$\mathbf{r}_A = (x_A, 0, 0), \quad (2.1-7)$$

and as a result,

$$A(f, \mathbf{r}_A) = A(f, x_A, y_A, z_A) \rightarrow A(f, x_A) \delta(y_A) \delta(z_A). \quad (2.1-8)$$

Therefore, by substituting (2.1-8) into (2.1-1) and using the sifting property of impulse functions, we obtain the following one-dimensional spatial Fourier transform for the far-field beam pattern of a linear aperture lying along the X axis:

$$D(f, f_X) = F_{x_A} \{ A(f, x_A) \} = \int_{-L/2}^{L/2} A(f, x_A) \exp(+j2\pi f_X x_A) dx_A \quad (2.1-9)$$

where

$$A(f, x_A) = a(f, x_A) \exp[+j\theta(f, x_A)] \quad (2.1-10)$$

is the complex frequency response (complex aperture function) of the linear aperture and

$$f_X = u/\lambda = \sin\theta \cos\psi/\lambda \quad (2.1-11)$$

is a spatial frequency in the X direction with units of cycles per meter [see (1.2-43)]. Since f_X can be expressed in terms of the spherical angles θ and ψ , the far-field beam pattern can ultimately be expressed as a function of frequency f and the spherical angles θ and ψ , that is, $D(f, f_X) \rightarrow D(f, \theta, \psi)$. If the linear aperture is a transmit aperture, then the aperture function $A(f, x_A)$ has units of $(m^3/sec)/V$ and the far-field beam pattern $D(f, f_X)$ has units of $(m^3/sec)/V$. However, if the linear aperture is a receive aperture, then $A(f, x_A)$ has units of $(V/(m^2/sec))/m$ and $D(f, f_X)$ has units of $V/(m^2/sec)$. These units are summarized in Table 2.1-1. In addition to describing the performance of an electroacoustic transducer by its far-field beam pattern, values of the frequency-dependent, *transmitter* and *receiver sensitivity functions* are also used. The relationships between the complex frequency response $A(f, x_A)$ of a single electroacoustic transducer, and complex, transmitter and receiver sensitivity functions are discussed in Appendix 2A.

Finally, if a linear aperture lies along either the Y or Z axis instead of the X axis, then simply replace x_A and f_X with either y_A and f_Y , or z_A and f_Z , respectively, in (2.1-9), where spatial frequencies f_Y and f_Z are given by (1.2-44)

Table 2.1-1 Units of the Complex Aperture Function $A(f, x_A)$ and Corresponding Far-Field Beam Pattern $D(f, f_X)$ for a Linear Aperture

Linear Aperture	$A(f, x_A)$	$D(f, f_X)$
transmit	$\left(\left(m^3/sec\right)/V\right)/m$	$(m^3/sec)/V$
receive	$\left(V/\left(m^2/sec\right)\right)/m$	$V/\left(m^2/sec\right)$

and (1.2-45), respectively. With the use of (2.1-9), we will derive closed-form expressions for the normalized, far-field beam patterns of six different amplitude windows in [Section 2.2](#). Although we shall be concentrating on single, continuous line sources and receivers in this chapter, as we shall discover in [Chapter 6](#), some of the results obtained in this chapter are directly applicable to linear arrays. In other words, we are laying the foundation for linear array theory in this chapter as well.

2.2 Amplitude Windows and Corresponding Far-Field Beam Patterns

The various amplitude windows to be discussed next are used to model the frequency response of linear apertures. They are very common functions used in sonar, radar, and communication problems and will serve our purposes of demonstrating far-field beam-pattern derivations, beamwidth calculations, and the relationship between beamwidth and sidelobe levels of far-field beam patterns. Sampled versions of these continuous amplitude windows are, in fact, used to amplitude weight arrays of electroacoustic transducers, as will be discussed in [Section 6.2](#). In addition, time-domain versions of these continuous amplitude windows can also be used to reduce the sidelobe levels of the auto-ambiguity functions of common transmitted electrical signals, as will be discussed in [Chapter 13](#).

In the subsections that follow, it is assumed that the linear aperture represents a single electroacoustic transducer – a continuous line source or receiver – L meters in length, and that the phase response of the transducer is zero so that

$$A(f, x_A) = a(f, x_A), \quad \theta(f, x_A) = 0. \quad (2.2-1)$$

Therefore, according to (2.2-1), the complex frequency response of the transducer is equal to the amplitude response or amplitude window $a(f, x_A)$. We will examine the effects of a nonzero phase response later, in [Section 2.4](#).

2.2.1 The Rectangular Amplitude Window

In this subsection we shall derive the normalized, far-field beam pattern of the rectangular amplitude window. The rectangular amplitude window is defined as follows:

$$a(f, x_A) = A_A \operatorname{rect}\left(\frac{x_A}{L}\right) \triangleq \begin{cases} A_A, & |x_A| \leq L/2 \\ 0, & |x_A| > L/2 \end{cases} \quad (2.2-2)$$

and is shown in Fig. 2.2-1 for $A_A = 1$. Therefore, if

$$A(f, x_A) = a(f, x_A) = A_A \operatorname{rect}(x_A/L), \quad (2.2-3)$$

then the complex frequency response of the transducer is constant along the entire length L of the transducer, regardless of the value of frequency f . The *real, positive* constant A_A carries the correct units of $A(f, x_A)$ (see Table 2.1-1). It is important to note that although A_A is shown here as a constant (and in Subsections 2.2.2 through 2.2.4), it is, in general, a *real, nonnegative* function of frequency, that is, $A_A \rightarrow A_A(f)$. Equation (2.2-3) is the simplest mathematical model for the complex aperture function $A(f, x_A)$.

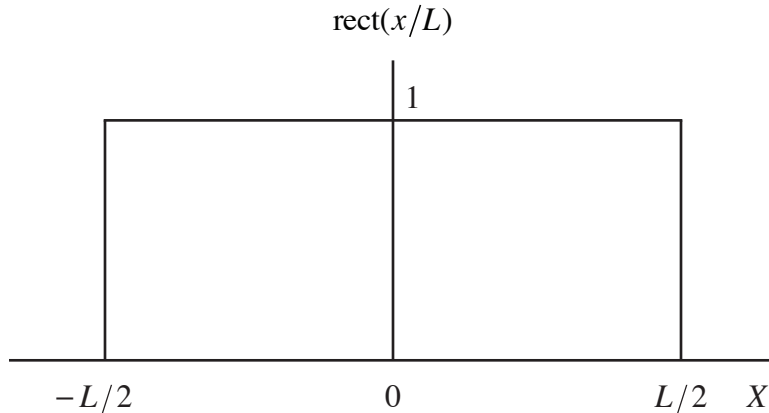


Figure 2.2-1 Rectangular amplitude window for $A_A = 1$.

Substituting (2.2-3) and (2.2-2) into (2.1-9) yields

$$D(f, f_X) = F_{x_A} \{A_A \operatorname{rect}(x_A/L)\} = A_A \int_{-L/2}^{L/2} \exp(+j2\pi f_X x_A) dx_A, \quad (2.2-4)$$

or

$$D(f, f_X) = F_{x_A} \{ A_A \text{rect}(x_A/L) \} = A_A L \text{sinc}(f_X L) \quad (2.2-5)$$

where

$$\text{sinc}(x) \triangleq \frac{\sin(\pi x)}{\pi x}. \quad (2.2-6)$$

Equation (2.2-5) is the *unnormalized*, far-field beam pattern of the rectangular amplitude window. The *dimensionless, normalized*, far-field beam pattern is defined as follows:

$$D_N(f, f_X) \triangleq D(f, f_X) / D_{\max} \quad (2.2-7)$$

where $D_{\max} = \max |D(f, f_X)|$ is the *normalization factor* – it is the *maximum* value of the *magnitude* of the unnormalized, far-field beam pattern. Therefore, by referring to (2.2-5),

$$|D(f, f_X)| = A_A L |\text{sinc}(f_X L)|, \quad (2.2-8)$$

and since $\text{sinc}(0) = 1$ is the maximum value of the sinc function,

$$D_{\max} = |D(f, 0)| = A_A L. \quad (2.2-9)$$

Dividing (2.2-5) by (2.2-9) yields the following expression for the *normalized*, far-field beam pattern of the rectangular amplitude window:

$$D_N(f, f_X) = \text{sinc}(f_X L) \quad (2.2-10)$$

Note that $|D_N(f, 0)| = 1$. Since $f_X = u/\lambda$, (2.2-10) can also be expressed as

$$D_N(f, u) = \text{sinc}\left(\frac{L}{\lambda} u\right) \quad (2.2-11)$$

where the wavelength λ was suppressed in the argument of D_N since frequency f and wavelength λ are related by $c = f\lambda$, that is, $D_N(f, f_X) = D_N(f, u/\lambda) \rightarrow D_N(f, u)$. The magnitude of the normalized, far-field beam pattern given by (2.2-11) is plotted as a function of direction cosine u in Fig. 2.2-2. The plot is shown only for positive values of u because the magnitude of the beam pattern is symmetric about $u = 0$. The level of the first sidelobe is approximately -13.3 dB.

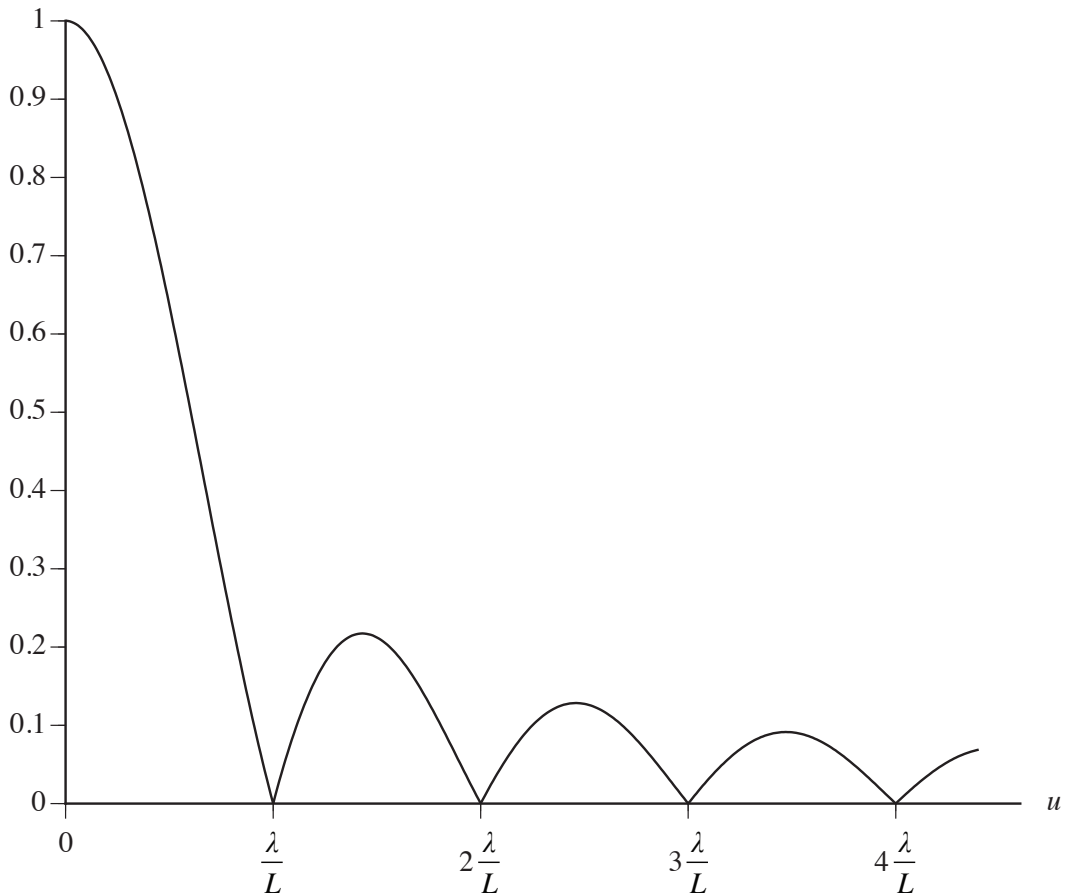
$|D_N(f, u)|$


Figure 2.2-2 Magnitude of the normalized, far-field beam pattern of the rectangular amplitude window plotted as a function of direction cosine u .

From Fig. 2.2-2 it can be seen that the width of the mainlobe of the normalized (and unnormalized), far-field beam pattern depends on the ratio λ/L . Therefore, the beamwidth is directly proportional to wavelength λ (inversely proportional to frequency f) and inversely proportional to the length L of the aperture (transducer). As a result, the beamwidth can be decreased by keeping the length L of the aperture constant while increasing frequency f , or by keeping frequency f constant while increasing the length L of the aperture. Beamwidth will be discussed in detail in Sections 2.3 and 2.5.

From a theoretical point of view, the normalized, far-field beam pattern given by (2.2-11) can be evaluated at any value of u . However, it is only the interval $-1 \leq u \leq 1$ that pertains to the real aperture problem because u is a direction cosine given by

$$u = \sin \theta \cos \psi , \quad (2.2-12)$$

and as a result, $-1 \leq u \leq 1$ since $0^\circ \leq \theta \leq 180^\circ$ and $0^\circ \leq \psi \leq 360^\circ$. The interval $-1 \leq u \leq 1$ is called the *visible region* of an aperture (transducer) lying along the X axis. The value $u = 0$, which implies that $\psi = 90^\circ$ or $\psi = 270^\circ$, corresponds to a field point being at *broadside* relative to an aperture (transducer) lying along the X axis (see Fig. 2.1-1). And $u = \pm 1$, which implies that $\theta = 90^\circ$ and $\psi = 0^\circ$ for $u = 1$; and $\theta = 90^\circ$ and $\psi = 180^\circ$ for $u = -1$; corresponds to a field point being at *end-fire* relative to an aperture (transducer) lying along the X axis (see Fig. 2.1-1).

With the use of (2.2-12), the normalized, far-field beam pattern of the rectangular amplitude window given by (2.2-11) can finally be expressed as

$$D_N(f, \theta, \psi) = \text{sinc}\left(\frac{L}{\lambda} \sin \theta \cos \psi\right) \quad (2.2-13)$$

By setting $\theta = 90^\circ$ in (2.2-13), we obtain

$$D_N(f, 90^\circ, \psi) = \text{sinc}\left(\frac{L}{\lambda} \cos \psi\right), \quad (2.2-14)$$

which is the normalized, *horizontal*, far-field beam pattern of the rectangular amplitude window (see Fig. 2.2-3). As can be seen from Fig. 2.2-3, as the ratio L/λ decreases (λ/L increases), the beamwidth increases. In other words, as the length of the aperture becomes small compared to the wavelength, the aperture acts like an omnidirectional transducer, that is, the magnitude of the normalized, horizontal, far-field beam pattern approaches being equal to one for all values of bearing angle. Horizontal beam patterns are discussed further in Example 2.3-2.

2.2.2 The Triangular Amplitude Window

In this subsection we shall derive the normalized, far-field beam pattern of the triangular amplitude window. The triangular amplitude window (also known as the Bartlett or Fejer window) is defined as follows:

$$a(f, x_A) = A_A \text{tri}\left(\frac{x_A}{L}\right) \triangleq \begin{cases} A_A \left[1 - \frac{|x_A|}{L/2}\right], & |x_A| \leq L/2 \\ 0, & |x_A| > L/2 \end{cases} \quad (2.2-15)$$

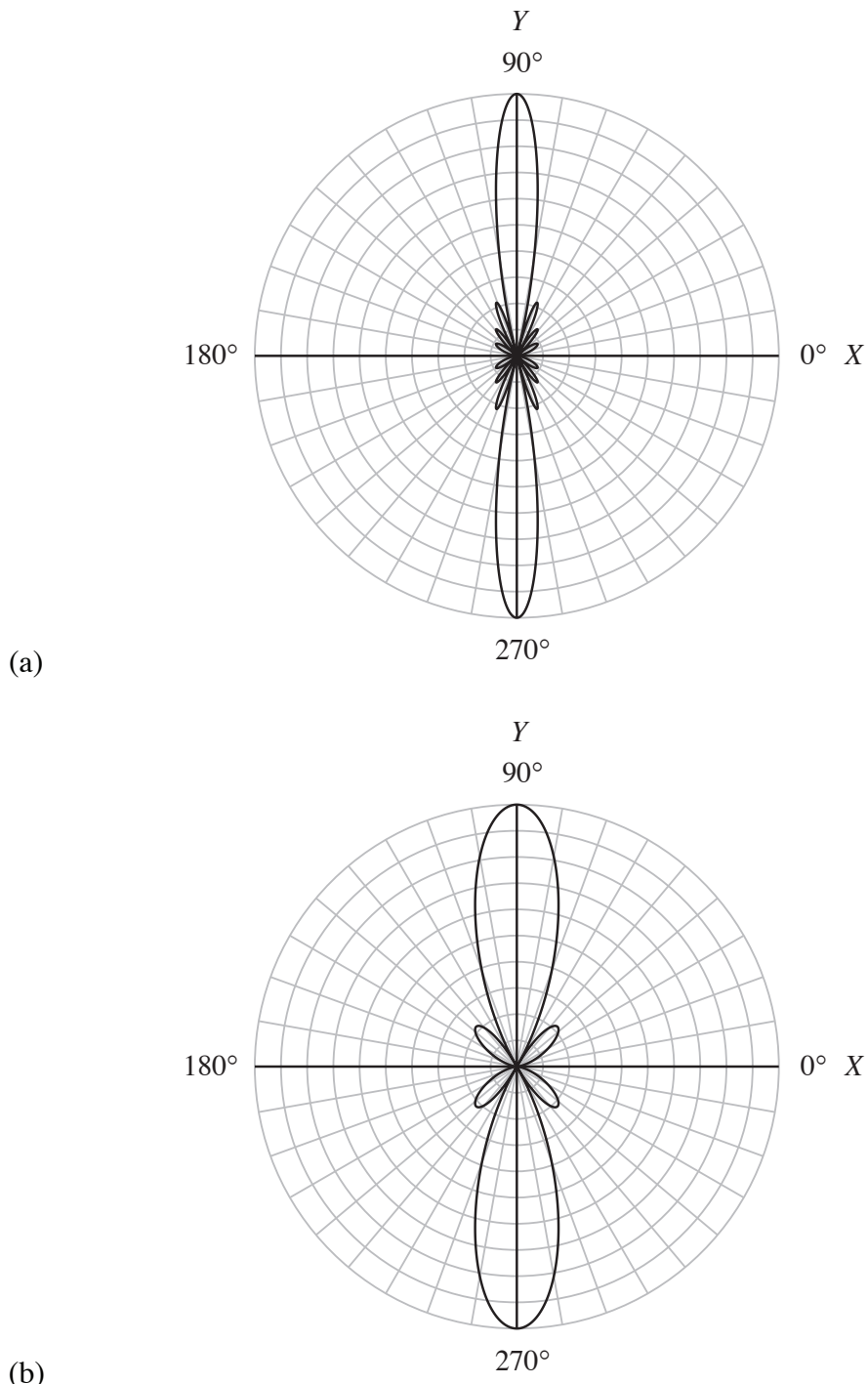
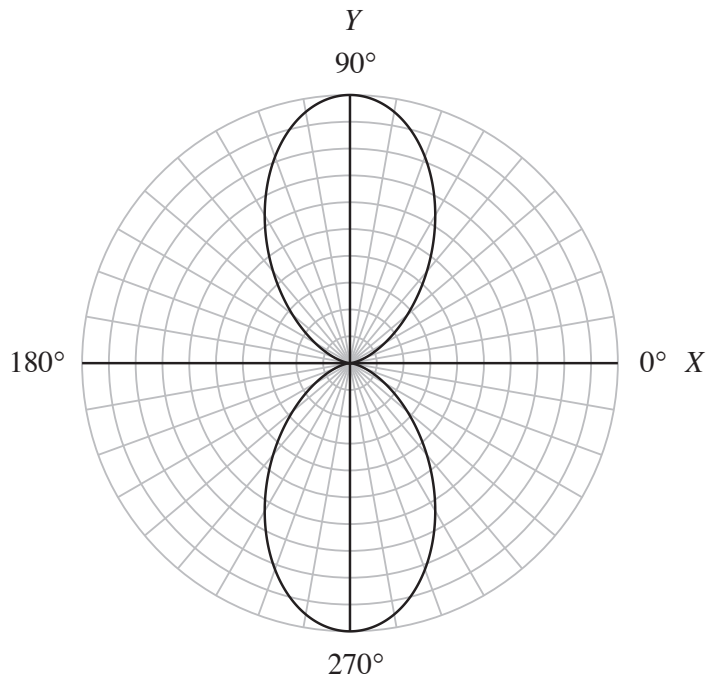
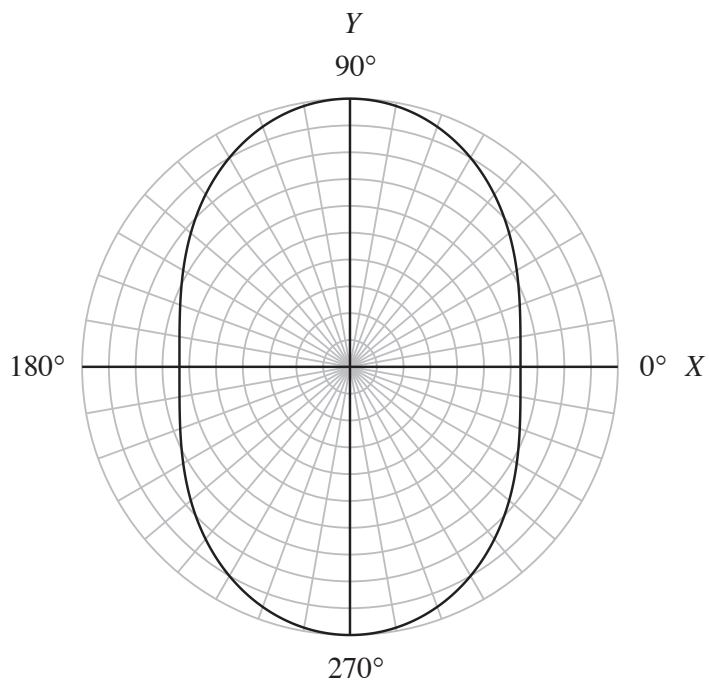


Figure 2.2-3 Polar plots as a function of the azimuthal (bearing) angle ψ of the magnitude of the normalized, horizontal, far-field beam pattern of the rectangular amplitude window given by (2.2-14) for (a) $L/\lambda = 4$, (b) $L/\lambda = 2$, (c) $L/\lambda = 1$, and (d) $L/\lambda = 0.5$.



(c)



(d)

Figure 2.2-3 continued.

and is shown in Fig. 2.2-4 for $A_A = 1$. Therefore, if

$$A(f, x_A) = a(f, x_A) = A_A \text{tri}(x_A/L), \quad (2.2-16)$$

then the complex frequency response of the transducer is triangular in shape along the length L of the transducer, regardless of the value of frequency f .

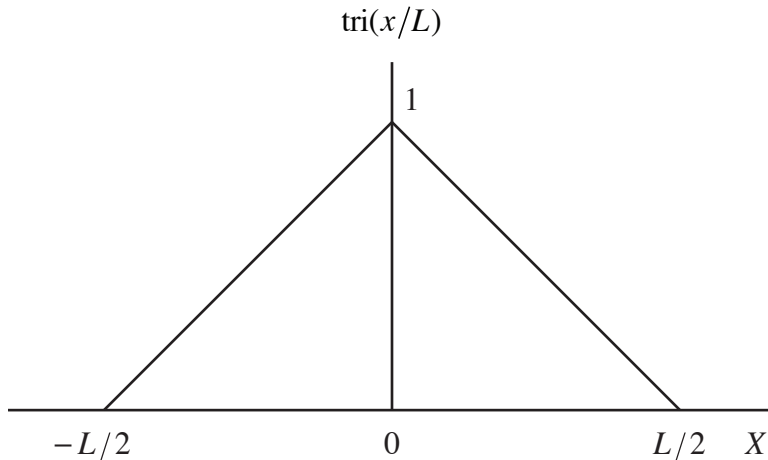


Figure 2.2-4 Triangular amplitude window for $A_A = 1$.

In order to derive the normalized, far-field beam pattern of the triangular amplitude window, we shall use the fact that a triangle is equal to the convolution of two rectangles of equal lengths, that is,

$$L_1 \text{tri}\left(\frac{x_A}{2L_1}\right) = \text{rect}\left(\frac{x_A}{L_1}\right) * \text{rect}\left(\frac{x_A}{L_1}\right). \quad (2.2-17)$$

Therefore,

$$F_{x_A} \left\{ L_1 \text{tri}\left(\frac{x_A}{2L_1}\right) \right\} = \left[F_{x_A} \left\{ \text{rect}\left(\frac{x_A}{L_1}\right) \right\} \right]^2 = L_1^2 \text{sinc}^2(f_X L_1), \quad (2.2-18)$$

or

$$F_{x_A} \left\{ A_A \text{tri}\left(\frac{x_A}{2L_1}\right) \right\} = A_A L_1 \text{sinc}^2(f_X L_1). \quad (2.2-19)$$

If we let $L_1 = L/2$, then (2.2-19) reduces to

$$D(f, f_x) = F_{x_A} \{ A_A \operatorname{tri}(x_A/L) \} = (A_A L/2) \operatorname{sinc}^2(f_x L/2) \quad (2.2-20)$$

Equation (2.2-20) is the *unnormalized*, far-field beam pattern of the triangular amplitude window. The direct evaluation of the spatial Fourier transform of (2.2-16) is left as a homework problem. By referring to (2.2-20), the normalization factor is given by

$$D_{\max} = |D(f, 0)| = A_A L/2, \quad (2.2-21)$$

since $\operatorname{sinc}(0) = 1$ is the maximum value of the sinc function. Dividing (2.2-20) by (2.2-21) yields the following expression for the *normalized*, far-field beam pattern of the triangular amplitude window (see Fig. 2.2-5):

$$D_N(f, f_x) = \operatorname{sinc}^2(f_x L/2) \quad (2.2-22)$$

The levels of the first sidelobes of the magnitudes of the normalized, far-field beam patterns of the rectangular and triangular amplitude windows are approximately -13.3 dB and -26.5 dB, respectively. However, the mainlobe of the beam pattern of the triangular amplitude window is wider than the mainlobe of the beam pattern of the rectangular amplitude window (see Fig. 2.2-5). Note that whereas the rectangular amplitude window is *discontinuous* at the end points $x = \pm L/2$ (see Fig. 2.2-1), the triangular amplitude window approaches zero at $x = \pm L/2$ in a comparatively smooth fashion (see Fig. 2.2-4). As a general rule, the smoother an amplitude window approaches zero at the end points $x = \pm L/2$, the lower the sidelobe levels of its far-field beam pattern will be. The word “smoother” implies “with a smaller slope.” However, a reduction in sidelobe levels generally results in an increase in the width of the beam pattern’s mainlobe. This trend will become more apparent as we consider additional amplitude windows.

2.2.3 The Cosine Amplitude Window

In order to derive the normalized, far-field beam pattern of the cosine amplitude window, we shall first derive the far-field beam pattern of the following related aperture function:

$$A(f, x_A) = A_A \cos(2\pi x_A/d) \operatorname{rect}(x_A/L). \quad (2.2-23)$$

This function is shown in Fig. 2.2-6 for $A_A = 1$ and $L = 2.5d$, where d is the *spatial period* in meters. Equation (2.2-23) is analogous to a time-domain,

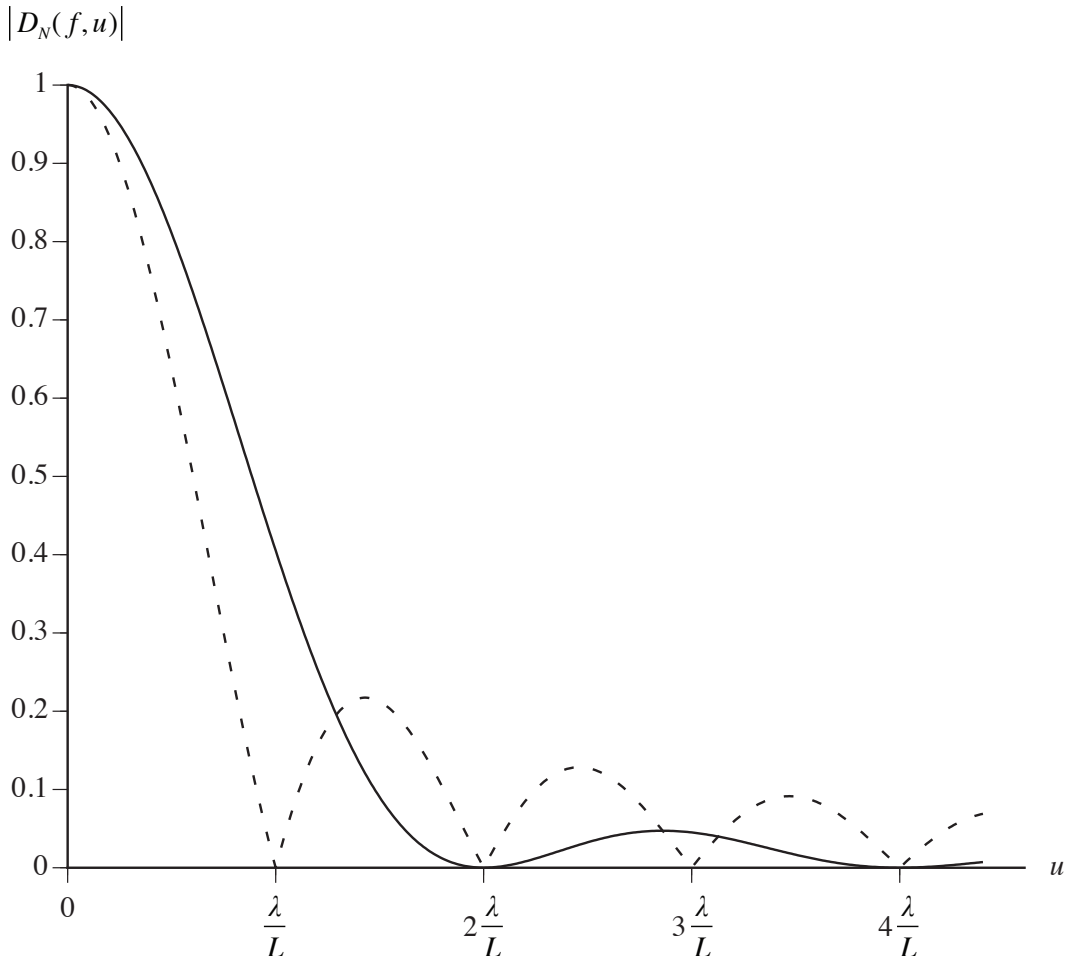


Figure 2.2-5 Magnitudes of the normalized, far-field beam patterns of the rectangular amplitude window (dashed curve) and triangular amplitude window (solid curve) plotted as a function of direction cosine u .

rectangular-envelope, continuous-wave (CW) pulse. Taking the spatial Fourier transform of (2.2-23) yields

$$\begin{aligned}
 D(f, f_X) &= F_{x_A} \left\{ A_A \cos(2\pi x_A/d) \text{rect}(x_A/L) \right\} \\
 &= A_A F_{x_A} \left\{ \cos(2\pi x_A/d) \right\} * F_{x_A} \left\{ \text{rect}(x_A/L) \right\}_{f_X} \\
 &= A_A L F_{x_A} \left\{ \cos(2\pi x_A/d) \right\} * \text{sinc}(f_X L),
 \end{aligned} \tag{2.2-24}$$

where use was made of (2.2-5).

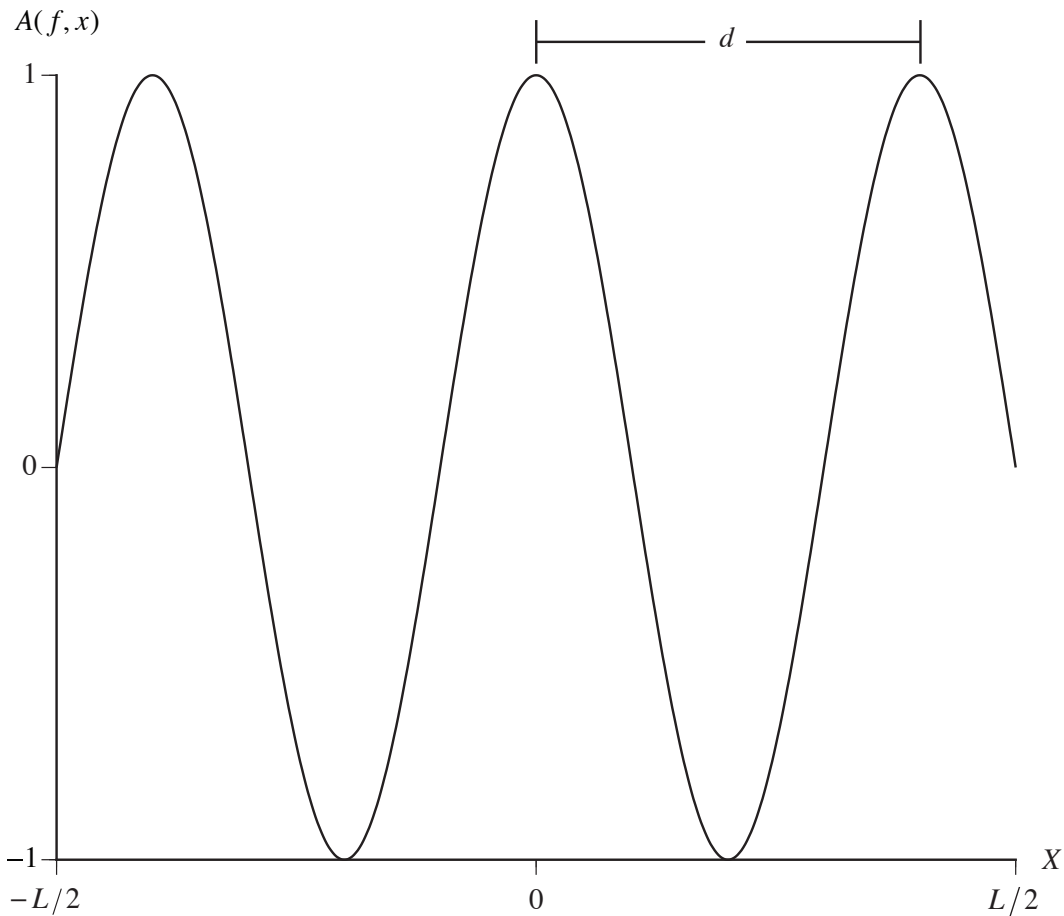


Figure 2.2-6 Plot of the aperture function given by (2.2-23) for $A_A=1$ and $L=2.5d$, where d is the spatial period in meters.

As can be seen from (2.2-24), what we need next is the spatial Fourier transform of the cosine function. Since

$$\cos(2\pi x_A/d) = 0.5[\exp(+j2\pi x_A/d) + \exp(-j2\pi x_A/d)] \quad (2.2-25)$$

and

$$F_{x_A}\{\exp(\pm j2\pi f'_X x_A)\} = \delta(f_X \pm f'_X), \quad (2.2-26)$$

$$F_{x_A}\{\cos(2\pi x_A/d)\} = \frac{1}{2} \left[\delta\left(f_X + \frac{1}{d}\right) + \delta\left(f_X - \frac{1}{d}\right) \right]. \quad (2.2-27)$$

Therefore, substituting (2.2-27) into (2.2-24) yields

$$\begin{aligned}
D(f, f_X) &= F_{x_A} \left\{ A_A \cos(2\pi x_A / d) \operatorname{rect}(x_A / L) \right\} \\
&= \frac{A_A L}{2} \left[\delta \left(f_X + \frac{1}{d} \right) + \delta \left(f_X - \frac{1}{d} \right) \right] * \operatorname{sinc}(f_X L) \\
&= \frac{A_A L}{2} \left[\delta \left(f_X + \frac{1}{d} \right) * \operatorname{sinc}(f_X L) + \delta \left(f_X - \frac{1}{d} \right) * \operatorname{sinc}(f_X L) \right],
\end{aligned} \tag{2.2-28}$$

or

$$\begin{aligned}
D(f, f_X) &= F_{x_A} \left\{ A_A \cos(2\pi x_A / d) \operatorname{rect}(x_A / L) \right\} \\
&= \frac{A_A L}{2} \left\{ \operatorname{sinc} \left[\left(f_X + \frac{1}{d} \right) L \right] + \operatorname{sinc} \left[\left(f_X - \frac{1}{d} \right) L \right] \right\}
\end{aligned} \tag{2.2-29}$$

The magnitude of the unnormalized, far-field beam pattern given by (2.2-29) is shown in Fig. 2.2-7 for $A_A = 1$ and $L = 2.5d$. Note that as $d \rightarrow \infty$, the aperture function given by (2.2-23) approaches $A_A \operatorname{rect}(x_A / L)$ and the beam pattern given by (2.2-29) approaches $A_A L \operatorname{sinc}(f_X L)$, which is the unnormalized, far-field beam pattern of the rectangular amplitude window. *Equation (2.2-29) is a very important result because it can be used to obtain the far-field beam patterns of the cosine, Hanning, Hamming, and Blackman amplitude windows, as we shall demonstrate next.*

The cosine amplitude window is given by

$$a(f, x_A) = A_A \cos(\pi x_A / L) \operatorname{rect}(x_A / L), \tag{2.2-30}$$

and is shown in Fig. 2.2-8 for $A_A = 1$. Therefore, if

$$A(f, x_A) = a(f, x_A) = A_A \cos(\pi x_A / L) \operatorname{rect}(x_A / L), \tag{2.2-31}$$

then the complex frequency response of the transducer is in the shape of a half-period cosine function along the length L of the transducer, regardless of the value of frequency f . Substituting $d = 2L$ into (2.2-29) and making use of the identity

$$\sin \left(\pi f_X L \pm \frac{\pi}{2} \right) = \pm \cos(\pi f_X L) \tag{2.2-32}$$

yields

$$D(f, f_X) = F_{x_A} \left\{ A_A \cos \left(\frac{\pi x_A}{L} \right) \operatorname{rect} \left(\frac{x_A}{L} \right) \right\} = \frac{2A_A L}{\pi} \frac{\cos(\pi f_X L)}{1 - (2f_X L)^2} \tag{2.2-33}$$

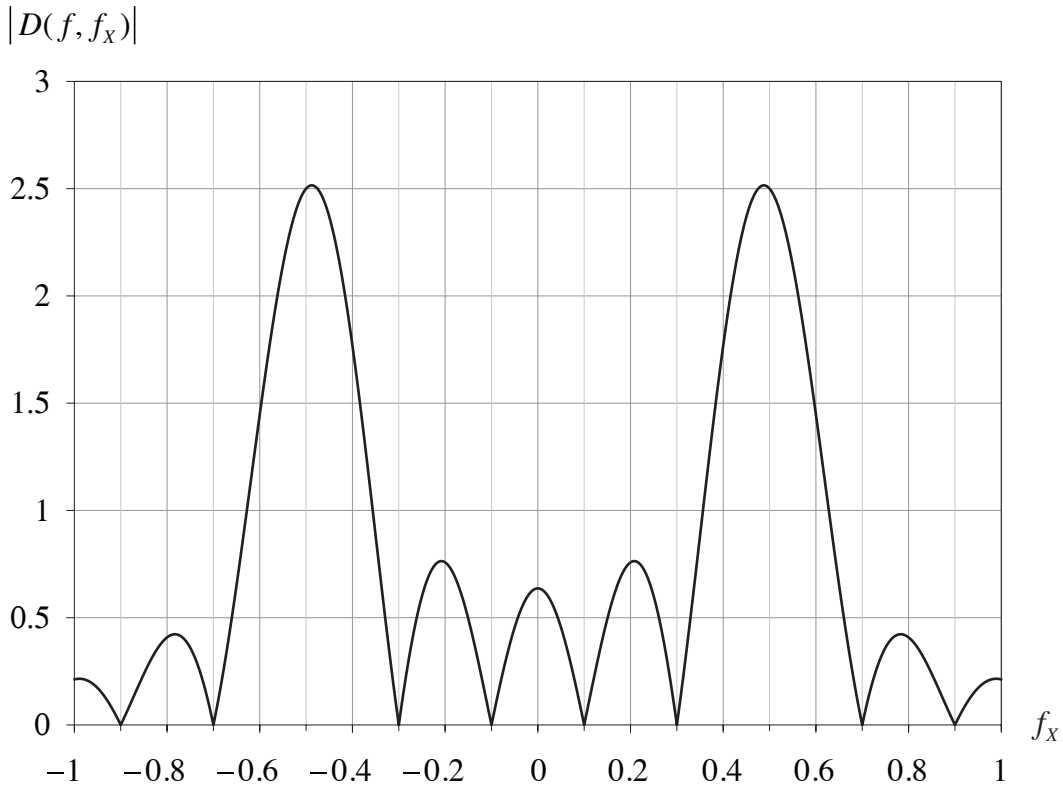


Figure 2.2-7 Magnitude of the unnormalized, far-field beam pattern given by (2.2-29) plotted as a function of spatial frequency f_x for $A_A=1$, $L=5\text{ m}$, and $d=2\text{ m}$ so that $L=2.5d$. Note that in this case, the maximum value of $|D(f, f_x)|$, which is slightly greater than $A_A L/2=2.5$, does not occur at $f_x=\pm 1/d=\pm 0.5\text{ cycles/m}$.

which is the *unnormalized*, far-field beam pattern of the cosine amplitude window. In order to determine the normalization factor for (2.2-33), we take advantage of the following general result: If the phase response $\theta(f, x_A)=0$ and the amplitude response (amplitude window) $a(f, x_A)\geq 0$, then the normalization factor $D_{\max}=|D(f, 0)|$ (see [Appendix 2D](#)). Therefore, by referring to (2.2-33),

$$D_{\max}=|D(f, 0)|=2A_A L/\pi. \quad (2.2-34)$$

Dividing (2.2-33) by (2.2-34) yields the following expression for the *normalized*, far-field beam pattern of the cosine amplitude window (see [Fig. 2.2-9](#)):

$$D_N(f, f_x)=\frac{\cos(\pi f_x L)}{1-(2f_x L)^2} \quad (2.2-35)$$

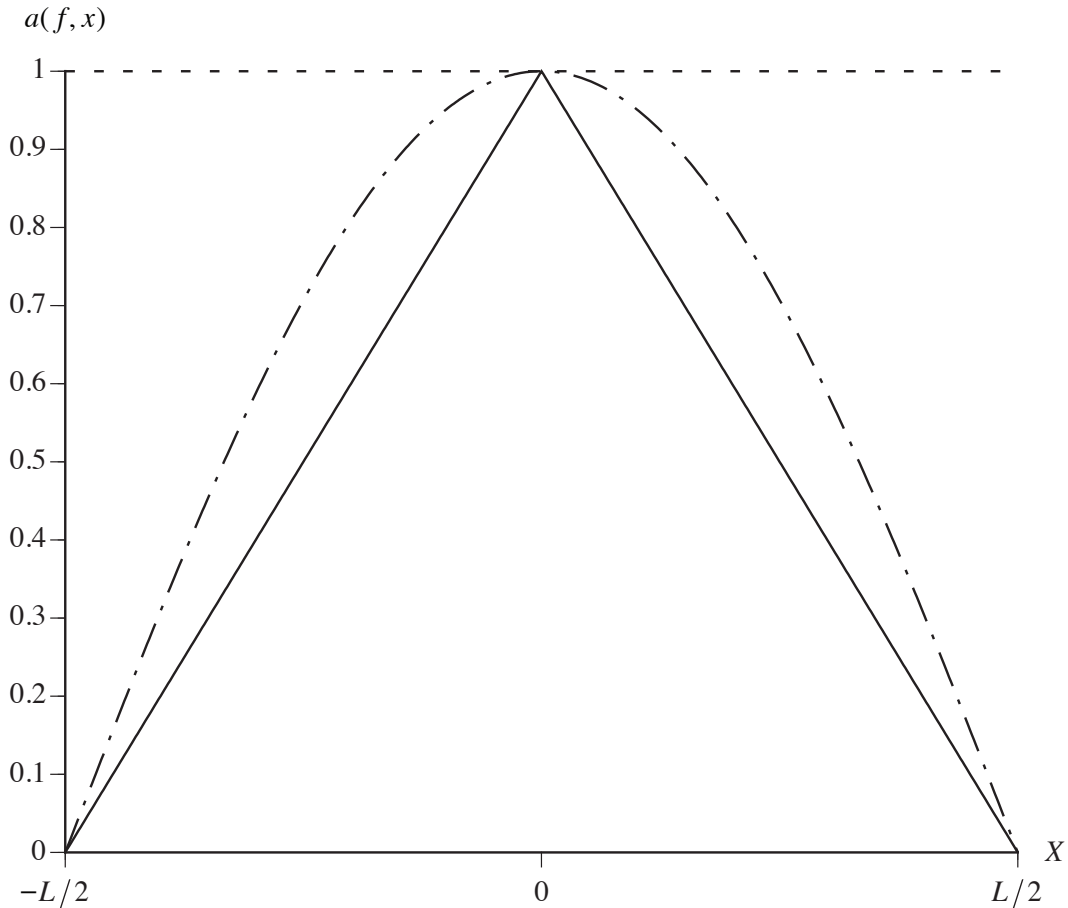


Figure 2.2-8 Rectangular amplitude window (dashed curve), triangular amplitude window (solid curve), and cosine amplitude window (dot-dash curve) for $A_A = 1$.

The level of the first sidelobe of the magnitude of the normalized, far-field beam pattern of the cosine amplitude window is approximately -23 dB, whereas the levels of the first sidelobes of the magnitudes of the normalized, far-field beam patterns of the rectangular and triangular amplitude windows are approximately -13.3 dB and -26.5 dB, respectively. This is not surprising since the rectangular amplitude window is discontinuous at the end points $x = \pm L/2$, and the cosine amplitude window approaches zero at the end points with a larger slope than the triangular amplitude window (see Fig. 2.2-8).

2.2.4 The Hanning, Hamming, and Blackman Amplitude Windows

The *Hanning* amplitude window, which is also known as the *cosine-*

$$|D_N(f, u)|$$

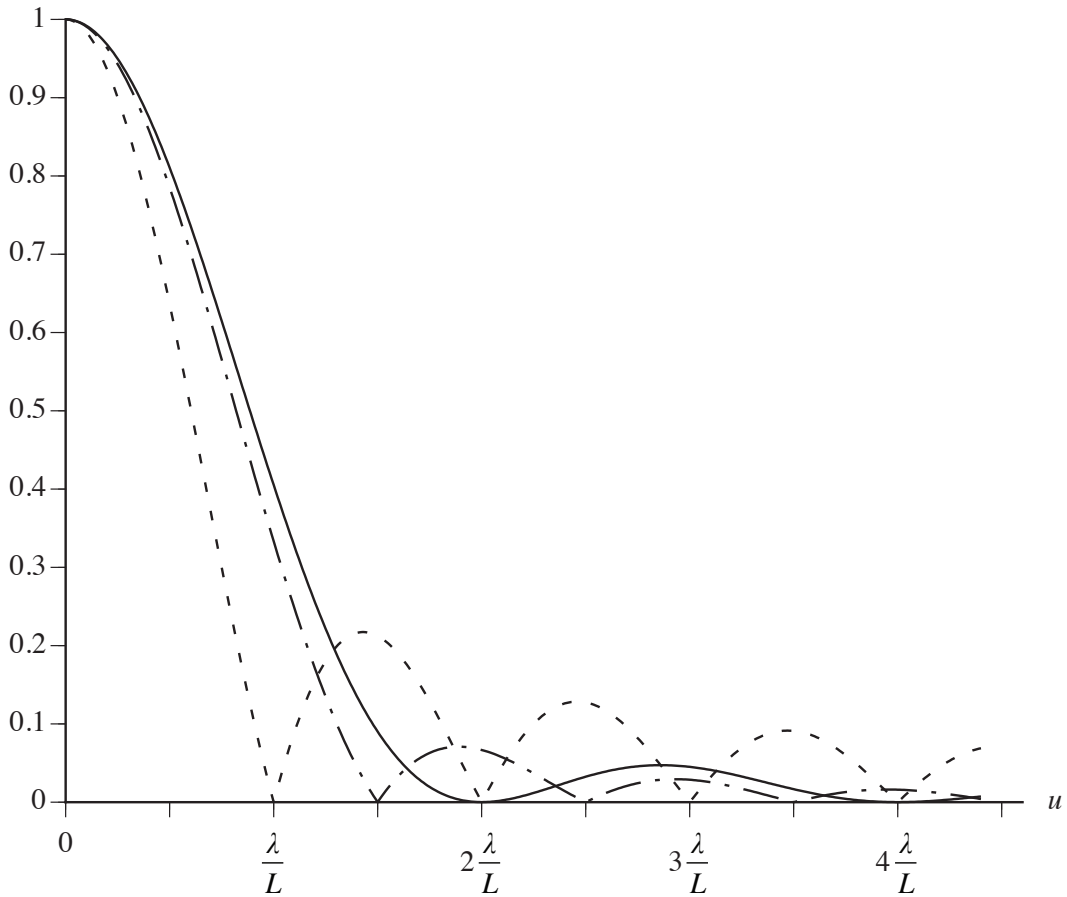


Figure 2.2-9 Magnitudes of the normalized, far-field beam patterns of the rectangular amplitude window (dashed curve), triangular amplitude window (solid curve), and cosine amplitude window (dot-dash curve) plotted as a function of direction cosine u .

squared or raised-cosine window, is given by

$$a(f, x_A) = A_A \cos^2(\pi x_A / L) \text{rect}(x_A / L), \quad (2.2-36)$$

and is shown in Fig. 2.2-10 for $A_A = 1$. Since

$$\cos^2 \alpha = 0.5 [1 + \cos(2\alpha)], \quad (2.2-37)$$

(2.2-36) can be rewritten as

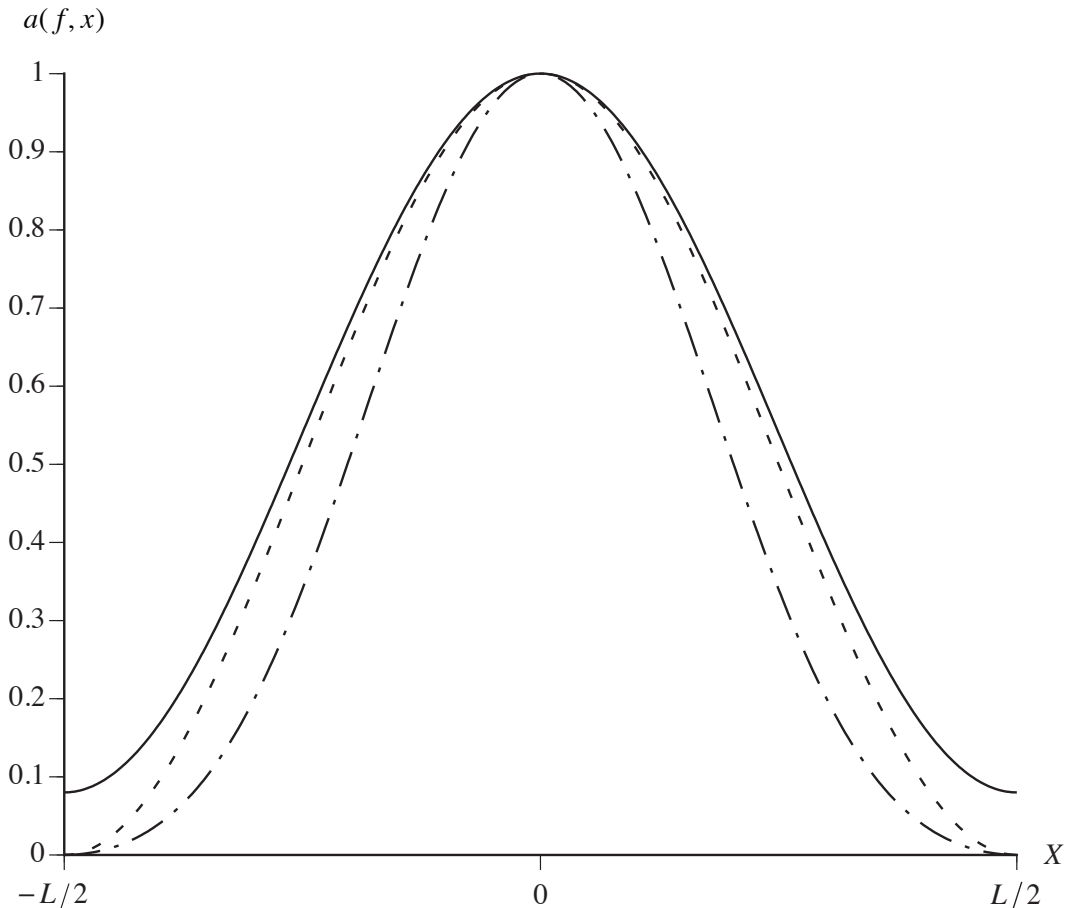


Figure 2.2-10 Hanning amplitude window (dashed curve), Hamming amplitude window (solid curve), and Blackman amplitude window (dot-dash curve) for $A_A = 1$.

$$a(f, x_A) = 0.5A_A [1 + \cos(2\pi x_A/L)] \text{rect}(x_A/L). \quad (2.2-38)$$

Therefore, if

$$A(f, x_A) = a(f, x_A) = 0.5A_A \text{rect}(x_A/L) + 0.5A_A \cos(2\pi x_A/L) \text{rect}(x_A/L), \quad (2.2-39)$$

then the complex frequency response of the transducer is in the shape of the Hanning amplitude window along the length L of the transducer, regardless of the value of frequency f .

The spatial Fourier transform of the first term on the right-hand side of (2.2-39) can be obtained by using (2.2-5), and the spatial Fourier transform of the second term can be obtained by substituting $d = L$ into (2.2-29). The unnormalized and normalized, far-field beam patterns of the Hanning amplitude

window are given by

$$D(f, f_x) = \frac{A_A L}{2} \frac{\text{sinc}(f_x L)}{1 - (f_x L)^2} \quad (2.2-40)$$

and

$$D_N(f, f_x) = \frac{\text{sinc}(f_x L)}{1 - (f_x L)^2} \quad (2.2-41)$$

respectively (see Fig. 2.2-11). The level of the first sidelobe of the magnitude of the normalized, far-field beam pattern of the Hanning amplitude window is approximately -31.5 dB.

The *Hamming* amplitude window is given by

$$a(f, x_A) = A_A [0.54 + 0.46 \cos(2\pi x_A / L)] \text{rect}(x_A / L), \quad (2.2-42)$$

and is shown in Fig. 2.2-10 for $A_A = 1$. Note that the Hamming amplitude window is discontinuous at the end points $x = \pm L/2$. Therefore, if

$$A(f, x_A) = a(f, x_A) = 0.54 A_A \text{rect}(x_A / L) + 0.46 A_A \cos(2\pi x_A / L) \text{rect}(x_A / L), \quad (2.2-43)$$

then the complex frequency response of the transducer is in the shape of the Hamming amplitude window along the length L of the transducer, regardless of the value of frequency f .

The spatial Fourier transform of the first term on the right-hand side of (2.2-43) can be obtained by using (2.2-5), and the spatial Fourier transform of the second term can be obtained by substituting $d = L$ into (2.2-29). The unnormalized and normalized, far-field beam patterns of the Hamming amplitude window are given by

$$D(f, f_x) = A_A L \frac{0.54 - 0.08(f_x L)^2}{1 - (f_x L)^2} \text{sinc}(f_x L) \quad (2.2-44)$$

and

$$D_N(f, f_x) = \frac{1}{0.54} \frac{0.54 - 0.08(f_x L)^2}{1 - (f_x L)^2} \text{sinc}(f_x L) \quad (2.2-45)$$

respectively (see Fig. 2.2-11). The level of the first sidelobe of the magnitude of

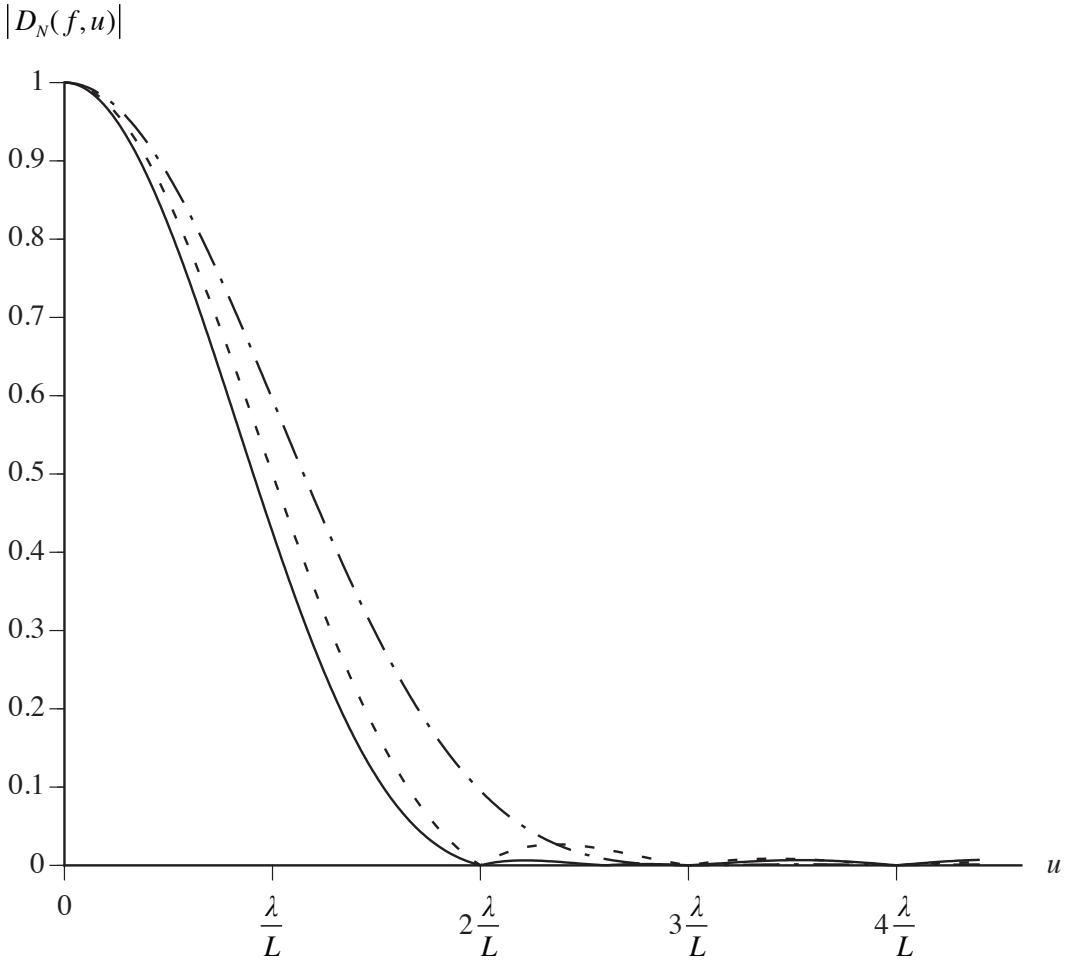


Figure 2.2-11 Magnitudes of the normalized, far-field beam patterns of the Hanning amplitude window (dashed curve), Hamming amplitude window (solid curve), and Blackman amplitude window (dot-dash curve) plotted as a function of direction cosine u .

the normalized, far-field beam pattern of the Hamming amplitude window is approximately -44 dB. From Fig. 2.2-11, it can be seen that although the level of the first sidelobe of the Hamming beam pattern is less than the level of the first sidelobe of the Hanning beam pattern, the width of the mainlobe of the Hamming beam pattern is also *less* than the width of the mainlobe of the Hanning beam pattern. This is an *exception* to the general rule that beamwidth increases as sidelobe levels decrease.

The *Blackman* amplitude window is given by

$$a(f, x_A) = A_A [0.42 + 0.5 \cos(2\pi x_A/L) + 0.08 \cos(4\pi x_A/L)] \text{rect}(x_A/L), \quad (2.2-46)$$

and is shown in [Fig. 2.2-10](#) for $A_A = 1$. Therefore, if

$$\begin{aligned} A(f, x_A) &= a(f, x_A) \\ &= 0.42A_A \operatorname{rect}(x_A/L) + 0.5A_A \cos(2\pi x_A/L) \operatorname{rect}(x_A/L) + \\ &\quad 0.08A_A \cos(4\pi x_A/L) \operatorname{rect}(x_A/L), \end{aligned} \quad (2.2-47)$$

then the complex frequency response of the transducer is in the shape of the Blackman amplitude window along the length L of the transducer, regardless of the value of frequency f .

The spatial Fourier transform of the first term on the right-hand side of (2.2-47) can be obtained by using (2.2-5), and the spatial Fourier transforms of the second and third terms can be obtained by substituting $d = L$ and $d = L/2$ into (2.2-29), respectively. The unnormalized and normalized, far-field beam patterns of the Blackman amplitude window are given by

$$D(f, f_x) = A_A L \frac{1.68 - 0.18(f_x L)^2}{[1 - (f_x L)^2][4 - (f_x L)^2]} \operatorname{sinc}(f_x L) \quad (2.2-48)$$

and

$$D_N(f, f_x) = \frac{1}{0.42} \frac{1.68 - 0.18(f_x L)^2}{[1 - (f_x L)^2][4 - (f_x L)^2]} \operatorname{sinc}(f_x L) \quad (2.2-49)$$

respectively (see [Fig. 2.2-11](#)). The level of the first sidelobe of the magnitude of the normalized, far-field beam pattern of the Blackman amplitude window is approximately -58.1 dB.

All of the amplitude windows discussed in [Section 2.2](#) were *even* functions of spatial variable x_A . As a result, their far-field beam patterns were *real, even* functions of spatial frequency f_x (direction cosine u). In general, if an amplitude window is an *even* function of a spatial variable, then the corresponding far-field beam pattern will be a *real, even* function of the appropriate spatial frequency (direction cosine) (see [Appendix 2C](#)). Similarly, if an amplitude window is an *odd* function of a spatial variable, then the corresponding far-field beam pattern will be an *imaginary, odd* function of the appropriate spatial frequency (direction cosine) (see [Appendix 2C](#)). Furthermore, if the phase response $\theta(f, x_A) = 0$ and the amplitude response (amplitude window) $a(f, x_A) \geq 0$, then the maximum value of the magnitude of the corresponding unnormalized, far-field beam pattern is at broadside. Therefore, the normalization factor in this case is $D_{\max} = |D(f, 0)|$ (see [Appendix 2D](#)). However,

whether or not this is the case, D_{\max} can also be found by using the standard calculus approach for finding the maximum value of a function, or by using the formulas in [Appendix 2D](#).

A summary of the one-dimensional spatial Fourier transforms used in [Section 2.2](#) is presented in [Table 2E-1](#) in [Appendix 2E](#).

2.3 Beamwidth

The term “beamwidth” refers to some measure of the width of the mainlobe of a far-field beam pattern. *The beamwidth of a far-field beam pattern is the same whether the beam pattern is normalized or unnormalized.* However, it is customary to work with normalized, far-field beam patterns. The most common measure of beamwidth is the 3-dB beamwidth. Since the maximum value of the magnitude of a *normalized*, far-field beam pattern is equal to 1, or 0 dB, the 3-dB beamwidth in two-dimensional space is defined as the width of the mainlobe between those two points that correspond to magnitude values equal to $\sqrt{2}/2$, or -3 dB . Note that

$$20 \log_{10}(\sqrt{2}/2) = 10 \log_{10}(1/2) = -3.01 \text{ dB}. \quad (2.3-1)$$

The 3-dB beamwidth is also referred to as the *half-power beamwidth* [note the argument 1/2 in the middle expression in (2.3-1)]. [Figure 2.3-1](#) shows the magnitude of a typical normalized, far-field beam pattern of a linear aperture lying along the X axis, plotted as a function of direction cosine u . The dimensionless 3-dB beamwidth Δu in direction-cosine space is given by

$$\Delta u = u_+ - u_- > 0, \quad (2.3-2)$$

or, since the magnitude of the beam pattern is symmetric about $u = 0$,

$$\Delta u = 2u_+, \quad (2.3-3)$$

where $u_+ > 0$ and $u_- < 0$ as shown.

The problem now is to express the 3-dB beamwidth Δu in terms of the 3-dB beamwidths $\Delta\theta$ and $\Delta\psi$ associated with the spherical angles θ and ψ . Whereas Δu is dimensionless, $\Delta\theta$ and $\Delta\psi$ have units in *degrees*. Since $u = \sin\theta \cos\psi$, let (see [Fig. 2.3-2](#))

$$u_+ = \sin\theta_+ \cos\psi_+ > 0, \quad (2.3-4)$$

$$|D_N(f, u)|$$

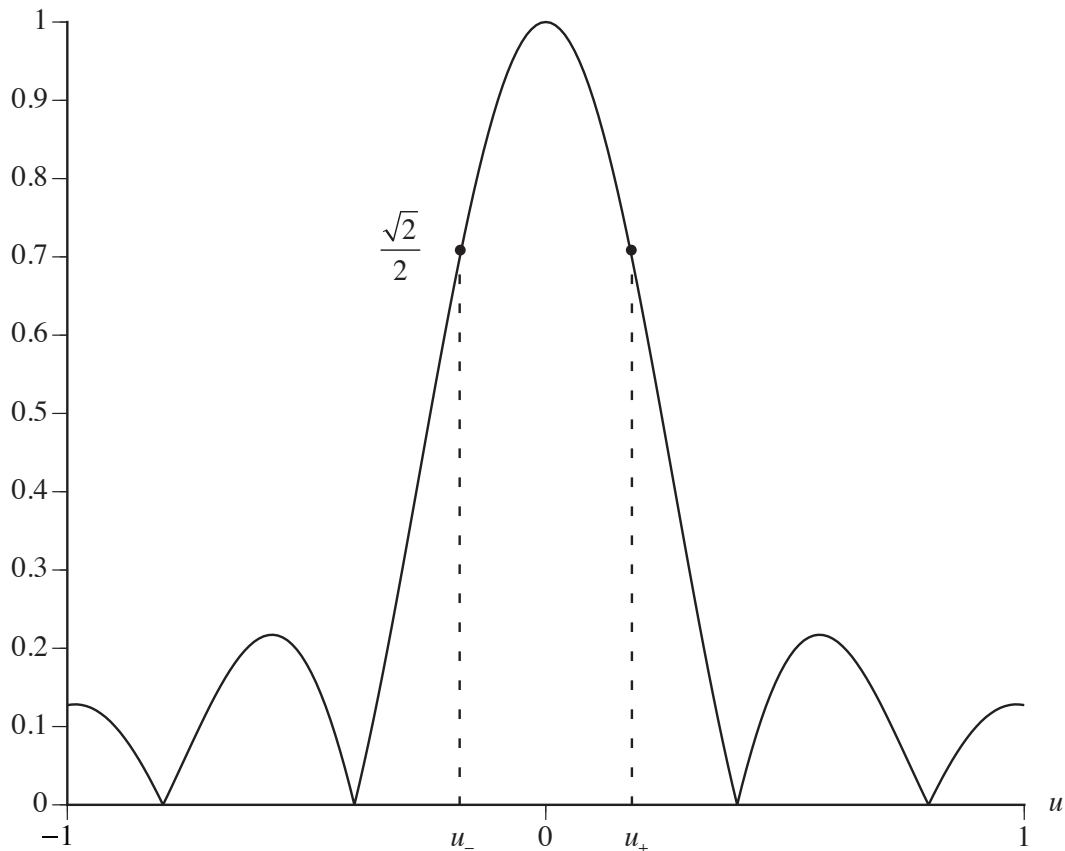


Figure 2.3-1 Magnitude of a typical normalized, far-field beam pattern of a linear aperture lying along the X axis, plotted as a function of direction cosine u .

where

$$\theta_+ = \Delta\theta/2 \quad (2.3-5)$$

and

$$\psi_+ = 90^\circ - \frac{\Delta\psi}{2}; \quad (2.3-6)$$

and let

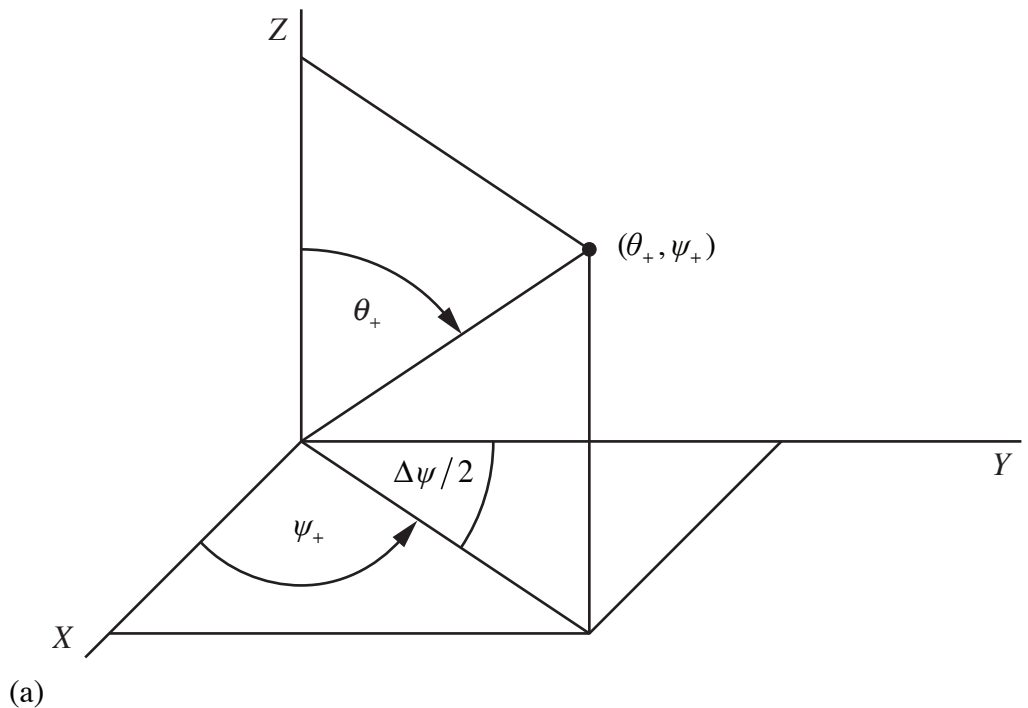
$$u_- = \sin\theta_- \cos\psi_- < 0, \quad (2.3-7)$$

where

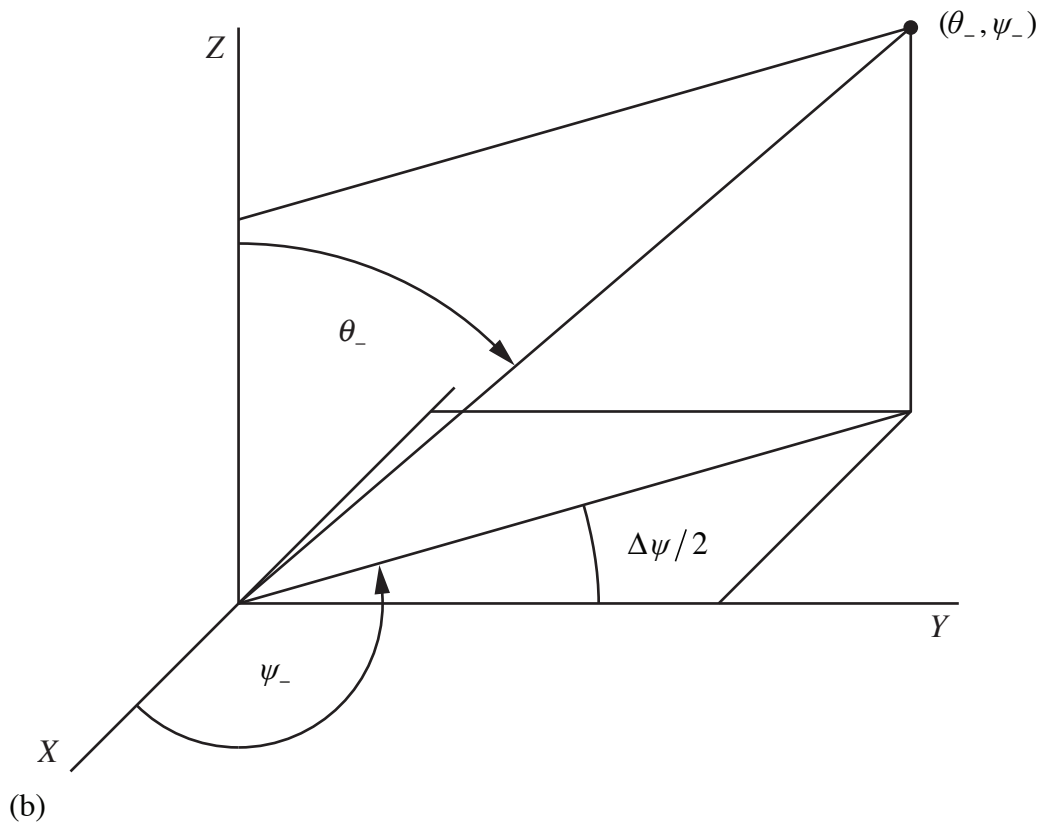
$$\theta_- = \theta_+ = \Delta\theta/2 \quad (2.3-8)$$

and

$$\psi_- = 90^\circ + \frac{\Delta\psi}{2}. \quad (2.3-9)$$



(a)



(b)

Figure 2.3-2 Representation of the spherical angles (a) (θ_+, ψ_+) and (b) (θ_-, ψ_-) .

With ψ_+ and ψ_- given by (2.3-6) and (2.3-9), respectively, it is assured that $u_+ > 0$ and $u_- < 0$ since

$$\cos \psi_+ = \cos\left(90^\circ - \frac{\Delta\psi}{2}\right) = \sin\left(\frac{\Delta\psi}{2}\right) > 0 \quad (2.3-10)$$

and

$$\cos \psi_- = \cos\left(90^\circ + \frac{\Delta\psi}{2}\right) = -\sin\left(\frac{\Delta\psi}{2}\right) < 0. \quad (2.3-11)$$

Substituting (2.3-5) and (2.3-10) into (2.3-4) yields

$$u_+ = \sin(\Delta\theta/2)\sin(\Delta\psi/2), \quad (2.3-12)$$

and substituting (2.3-8) and (2.3-11) into (2.3-7) yields

$$u_- = -\sin(\Delta\theta/2)\sin(\Delta\psi/2). \quad (2.3-13)$$

Finally, by substituting (2.3-12) and (2.3-13) into (2.3-2), we obtain

$$\Delta u = 2\sin(\Delta\theta/2)\sin(\Delta\psi/2). \quad (2.3-14)$$

However, we now have only *one equation* but *two unknowns*, $\Delta\theta$ and $\Delta\psi$. Therefore, when dealing with a linear aperture, we must restrict ourselves to either the *vertical* or *horizontal* far-field beam pattern when making a beamwidth calculation, as is demonstrated in the next two examples.

Example 2.3-1 Vertical Beam Pattern

Consider a linear aperture lying along the X axis. Therefore, by definition, the vertical beam pattern lies in the XZ plane (see Fig. 2.3-3). In the XZ plane, $u = \sin\theta$ when $\psi = 0^\circ$, and $u = -\sin\theta$ when $\psi = 180^\circ$. As a result,

$$u_+ = \sin\theta_+ > 0, \quad \psi_+ = 0^\circ, \quad (2.3-15)$$

and

$$u_- = -\sin\theta_- < 0, \quad \psi_- = 180^\circ, \quad (2.3-16)$$

where

$$\theta_+ = \theta_- = \Delta\theta/2. \quad (2.3-17)$$

Therefore,

$$\Delta u = u_+ - u_- = 2\sin(\Delta\theta/2) > 0, \quad (2.3-18)$$

or

$$\boxed{\Delta\theta = 2 \sin^{-1}(\Delta u/2), \quad \Delta u/2 \leq 1} \quad (2.3-19)$$

where $\Delta\theta$ is the 3-dB beamwidth in degrees of a vertical, far-field beam pattern in the XZ plane. ■

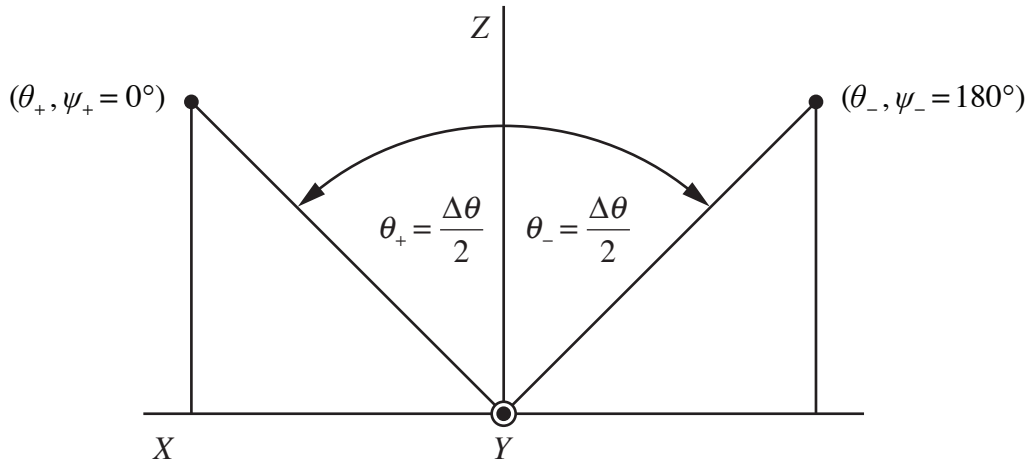


Figure 2.3-3 Representation of the spherical angles $(\theta_+, \psi_+ = 0^\circ)$ and $(\theta_-, \psi_- = 180^\circ)$.

Example 2.3-2 Horizontal Beam Pattern

Consider a linear aperture lying along the X axis. Therefore, by definition, the horizontal beam pattern lies in the XY plane (see Fig. 2.3-4). In the XY plane, $u = \cos\psi$ since $\theta = 90^\circ$. As a result,

$$u_+ = \cos\psi_+ > 0, \quad \theta_+ = 90^\circ, \quad (2.3-20)$$

and

$$u_- = \cos\psi_- < 0, \quad \theta_- = 90^\circ, \quad (2.3-21)$$

where

$$\psi_+ = 90^\circ - \frac{\Delta\psi}{2} \quad (2.3-22)$$

and

$$\psi_- = 90^\circ + \frac{\Delta\psi}{2}. \quad (2.3-23)$$

Therefore, with the use of (2.3-10) and (2.3-11),

$$\Delta u = u_+ - u_- = 2 \sin(\Delta\psi/2) > 0 , \quad (2.3-24)$$

or

$$\boxed{\Delta\psi = 2 \sin^{-1}(\Delta u/2), \quad \Delta u/2 \leq 1} \quad (2.3-25)$$

where $\Delta\psi$ is the 3-dB beamwidth in degrees of a horizontal, far-field beam pattern in the XY plane. Note that the right-hand sides of (2.3-19) and (2.3-25) are identical. ■

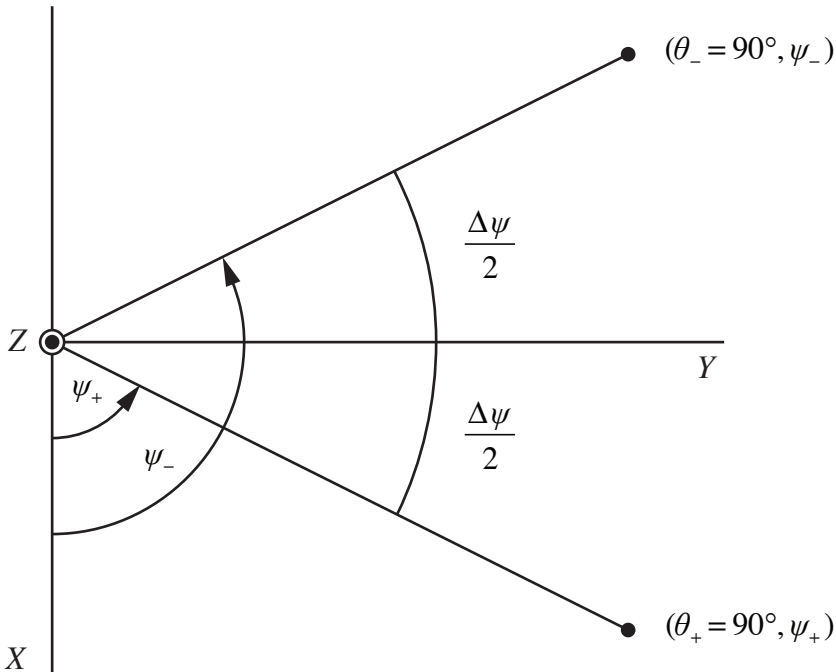


Figure 2.3-4 Representation of the spherical angles $(\theta_+ = 90^\circ, \psi_+)$ and $(\theta_- = 90^\circ, \psi_-)$.

By examining (2.3-19) and (2.3-25), it can be seen that in order to obtain numerical values for $\Delta\theta$ and $\Delta\psi$, we need to know Δu . Consider the next example.

Example 2.3-3

In this example we shall compute the 3-dB beamwidth Δu in direction-cosine space of the normalized, far-field beam pattern of the rectangular

amplitude window given by (2.2-11). Remember that the beamwidth of a far-field beam pattern is the same whether the beam pattern is normalized or unnormalized. With the use of (2.2-6), evaluating the magnitude of (2.2-11) at $u = u_+$ yields

$$|D_N(f, u_+)| = \left| \text{sinc}\left(\frac{L}{\lambda}u_+\right) \right| = \frac{\sin(\pi Lu_+/\lambda)}{\pi Lu_+/\lambda} = \frac{\sqrt{2}}{2} \quad (2.3-26)$$

since u_+ is the coordinate of one of the 3-dB-down points in direction-cosine space. Note that the absolute value operator was removed from $\sin(\pi Lu_+/\lambda)/(\pi Lu_+/\lambda)$ because this sinc function is positive when evaluated at u_+ . Equation (2.3-26) can be rewritten as

$$\sin(\pi x) - \frac{\sqrt{2}}{2}\pi x = 0, \quad (2.3-27)$$

where

$$x = \frac{L}{\lambda}u_+, \quad (2.3-28)$$

and by substituting (2.3-3) into (2.3-28), we obtain

$$\Delta u = 2x\lambda/L. \quad (2.3-29)$$

Since the solution (root) of (2.3-27) is $x \approx 0.443$, substituting this result into (2.3-29) yields

$$\boxed{\Delta u \approx 0.886\lambda/L} \quad (2.3-30)$$

for the rectangular amplitude window. Therefore, by substituting (2.3-30) into (2.3-19) and (2.3-25), the 3-dB beamwidths of the vertical and horizontal, far-field beam patterns of the rectangular amplitude window can be computed as functions of frequency (wavelength) and aperture length. It is important to note that this procedure can be used to calculate Δu for *any* normalized, far-field beam pattern of a linear aperture, including the normalized, far-field beam patterns of linear arrays. ■

[Table 2.3-1](#) summarizes the dimensionless 3-dB beamwidth Δu in direction-cosine space of the normalized, far-field beam patterns of the six different amplitude windows discussed in [Section 2.2](#). As was previously shown in [Fig. 2.2-11](#), and is also shown now in [Table 2.3-1](#), although the level of the first

sidelobe of the Hamming beam pattern is less than the level of the first sidelobe of the Hanning beam pattern, the width of the mainlobe of the Hamming beam pattern is also less than the width of the mainlobe of the Hanning beam pattern. This is an exception to the general rule that beamwidth increases as sidelobe levels decrease.

Table 2.3-1 The Dimensionless 3-dB Beamwidth Δu in Direction-Cosine Space of the Normalized, Far-Field Beam Patterns of Six Different Amplitude Windows

Amplitude Window	Level of 1st Sidelobe of the Magnitude of the Normalized Far-Field Beam Pattern (dB)	Δu
rectangular	-13.3	$0.886 \lambda/L$
cosine	-23.0	$1.189 \lambda/L$
triangular	-26.5	$1.276 \lambda/L$
Hanning	-31.5	$1.441 \lambda/L$
Hamming	-44.0	$1.303 \lambda/L$
Blackman	-58.1	$1.644 \lambda/L$

2.4 Beam Steering

In [Section 2.2](#) we assumed that the phase response of a linear aperture was equal to zero and concentrated our efforts on deriving closed-form expressions for the far-field beam patterns of various amplitude windows. In this section we shall study what happens to a far-field beam pattern when the phase response $\theta(f, x_A)$ is nonzero, in particular, when $\theta(f, x_A)$ is a linear function of x_A .

Let us begin the analysis by expressing $\theta(f, x_A)$ in terms of the following N th-order polynomial with frequency-dependent coefficients:

$$\theta(f, x_A) = \theta_0(f) + \theta_1(f)x_A + \theta_2(f)x_A^2 + \dots + \theta_N(f)x_A^N, \quad (2.4-1)$$

where for a given value of frequency f , $\theta_0(f)$ represents a *constant* value of phase (constant with respect to x_A) along the length of the aperture, $\theta_1(f)x_A$ represents a *linear* phase response along the length of the aperture and is responsible for *beam steering (beam tilting)*, and $\theta_2(f)x_A^2$ represents a *quadratic* phase response along the length of the aperture and is responsible for *focusing* in the Fresnel region of the aperture. The remaining higher-order terms in (2.4-1) are not considered. Note that (2.4-1) could be used as a mathematical model if we were trying to fit a N th-order polynomial to actual phase response data using, for example, the method of nonlinear least-squares estimation.

Next, let $D(f, f_X)$ be the far-field beam pattern of the amplitude window $a(f, x_A)$:

$$D(f, f_X) = F_{x_A} \{a(f, x_A)\} = \int_{-\infty}^{\infty} a(f, x_A) \exp(+j2\pi f_X x_A) dx_A. \quad (2.4-2)$$

Let $D'(f, f_X)$ be the far-field beam pattern of the aperture function $A(f, x_A)$ given by (2.1-10):

$$\begin{aligned} D'(f, f_X) &= F_{x_A} \{a(f, x_A) \exp[+j\theta(f, x_A)]\} \\ &= \int_{-\infty}^{\infty} a(f, x_A) \exp[+j\theta(f, x_A)] \exp(+j2\pi f_X x_A) dx_A. \end{aligned} \quad (2.4-3)$$

Now let the phase response along the length of the aperture be a linear function of x_A , that is, let

$$\theta(f, x_A) = \theta_l(f) x_A, \quad (2.4-4)$$

where

$$\theta_l(f) = -2\pi f'_X, \quad (2.4-5)$$

$$f'_X = u'/\lambda = fu'/c, \quad (2.4-6)$$

and

$$u' = \sin \theta' \cos \psi'. \quad (2.4-7)$$

The linear phase response given by (2.4-4) is an *odd* function of x_A and is a *straight line* that passes through the origin with frequency-dependent slope given by (2.4-5). If (2.4-4) and (2.4-5) are substituted into (2.4-3), then

$$\begin{aligned} D'(f, f_X) &= F_{x_A} \{a(f, x_A) \exp(-j2\pi f'_X x_A)\} \\ &= \int_{-\infty}^{\infty} a(f, x_A) \exp[+j2\pi(f_X - f'_X)x_A] dx_A, \end{aligned} \quad (2.4-8)$$

and by comparing (2.4-8) with (2.4-2),

$$D'(f, f_X) = D(f, f_X - f'_X), \quad (2.4-9)$$

or

$$F_{x_A} \{a(f, x_A) \exp(-j2\pi f'_X x_A)\} = D(f, f_X - f'_X), \quad (2.4-10)$$

where $D(f, f_X)$ is given by (2.4-2). Equation (2.4-9) can also be expressed as

$$D'(f, u) = D(f, u - u') \quad (2.4-11)$$

since $D(f, f_X) = D(f, u/\lambda) \rightarrow D(f, u)$. Therefore, a linear phase response along the length of the aperture will cause the beam pattern $D(f, u)$ to be steered in the direction $u = u'$ in direction-cosine space, which is equivalent to steering (tilting) the beam pattern to $\theta = \theta'$ and $\psi = \psi'$ [see (2.4-7)]. Equation (2.4-11) indicates that the far-field beam pattern $D'(f, u)$ is simply a translated or shifted version of $D(f, u)$ along the u axis, implying that the shape and beamwidth of the mainlobe of the beam pattern remain unchanged (see Fig. 2.4-1). However, as we shall show in Section 2.5, when a beam pattern is steered, the shape and beamwidth of the mainlobe of the beam pattern *do change* when the magnitude of the beam pattern is plotted as a function of the spherical angles θ and ψ .

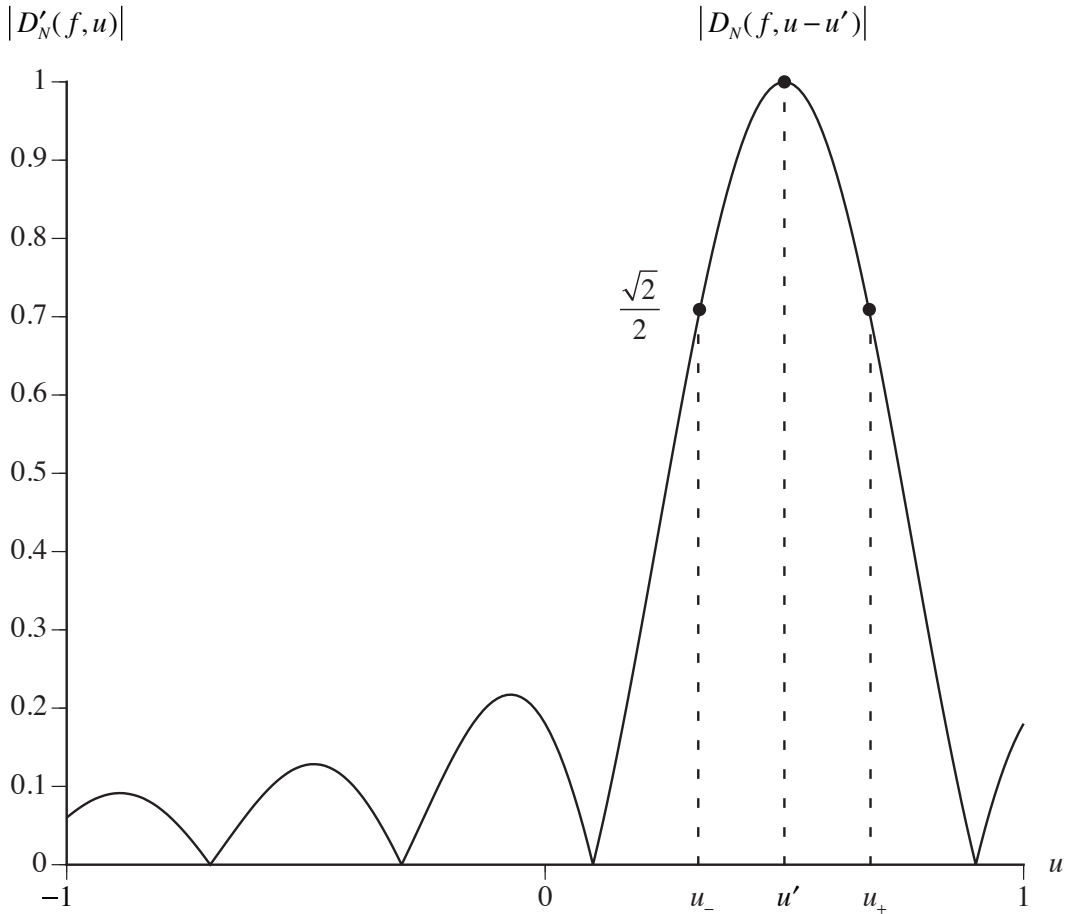


Figure 2.4-1 Magnitude of a typical normalized, far-field beam pattern of a linear aperture lying along the X axis, steered in the direction $u = u'$ in direction-cosine space.

2.5 Beamwidth at an Arbitrary Beam-Steer Angle

When a far-field beam pattern is steered (tilted) from broadside toward end-fire, its *beamwidth will increase from a minimum value at broadside to a maximum value at end-fire*.

In order to compute the beamwidth at an arbitrary beam-steer angle, let us restrict ourselves to the horizontal, far-field beam pattern of a linear aperture lying along the X axis (see Example 2.3-2), where ψ' is the beam-steer angle in the XY plane (see Fig. 2.5-1). In the XY plane, $u = \cos \psi$ since $\theta = 90^\circ$. Therefore, by referring to Figs. 2.4-1, 2.5-1, and 2.5-2,

$$u_+ = \cos \psi_+ > 0, \quad \theta_+ = 90^\circ, \quad (2.5-1)$$

$$u_- = \cos \psi_- > 0, \quad \theta_- = 90^\circ, \quad (2.5-2)$$

and

$$u' = \cos \psi' > 0, \quad \theta' = 90^\circ, \quad (2.5-3)$$

where

$$u_+ > u_-, \quad (2.5-4)$$

$$u_+ = u' + (\Delta u / 2), \quad (2.5-5)$$

and

$$u_- = u' - (\Delta u / 2). \quad (2.5-6)$$

Substituting (2.5-1) and (2.5-3) into (2.5-5) yields

$$\cos \psi_+ = \cos \psi' + (\Delta u / 2), \quad (2.5-7)$$

and by solving for ψ_+ we obtain

$$\psi_+ = \cos^{-1} [\cos \psi' + (\Delta u / 2)]. \quad (2.5-8)$$

Similarly, substituting (2.5-2) and (2.5-3) into (2.5-6) yields

$$\cos \psi_- = \cos \psi' - (\Delta u / 2), \quad (2.5-9)$$

and by solving for ψ_- we obtain

$$\psi_- = \cos^{-1} [\cos \psi' - (\Delta u / 2)]. \quad (2.5-10)$$

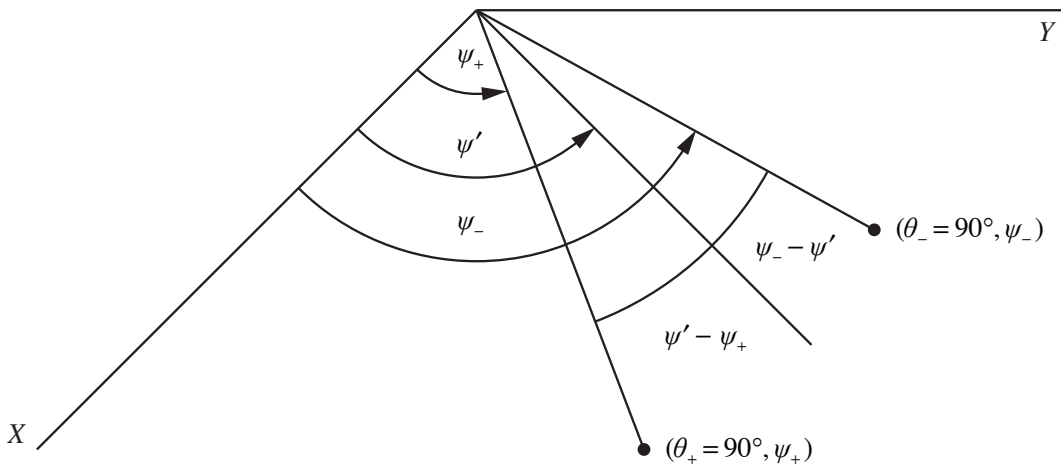


Figure 2.5-1 Representation of the spherical angles $(\theta_+ = 90^\circ, \psi_+)$, $(\theta_- = 90^\circ, \psi_-)$ and the beam-steer angle ψ' . Note that the *half-beamwidth angles* $\psi'_-\psi_+$ and $\psi_--\psi'$ are *not* equal in general.

From Figs. 2.5-1 and 2.5-2 it can be seen that the 3-dB beamwidth in degrees of a horizontal, far-field beam pattern in the XY plane is given by

$$\Delta\psi = \psi_- - \psi_+. \quad (2.5-11)$$

Substituting (2.5-8) and (2.5-10) into (2.5-11) yields

$$\Delta\psi = \cos^{-1}\left(\cos\psi' - \frac{\Delta u}{2}\right) - \cos^{-1}\left(\cos\psi' + \frac{\Delta u}{2}\right), \quad \left|\cos\psi' \pm \frac{\Delta u}{2}\right| \leq 1$$

(2.5-12)

where Δu can be obtained by using the procedure outlined in Example 2.3-3 (also see Table 2.3-1). In order to use (2.5-12), the inequality on the right-hand side must hold for both the plus and minus signs.

Although the *half-beamwidth angles* $\psi'_-\psi_+$ and $\psi_--\psi'$ are not equal, in general, for arbitrary beam-steer angles ψ' ; they are equal to one another and to $\Delta\psi/2$ for $\psi'=0^\circ$ (end-fire), 90° (broadside), 180° (end-fire), 270° (broadside), and 360° (end-fire) since $\cos\psi$ is symmetric about $\psi=\psi'=0^\circ$, 90° , 180° , 270° , and 360° (see Fig. 2.5-2). Note that $\psi'=90^\circ$ corresponds to an *unsteered* horizontal beam pattern for a linear aperture lying along the X axis (see Fig. 2.5-1). With $\psi'=90^\circ$, (2.5-12) reduces to (2.3-25) since

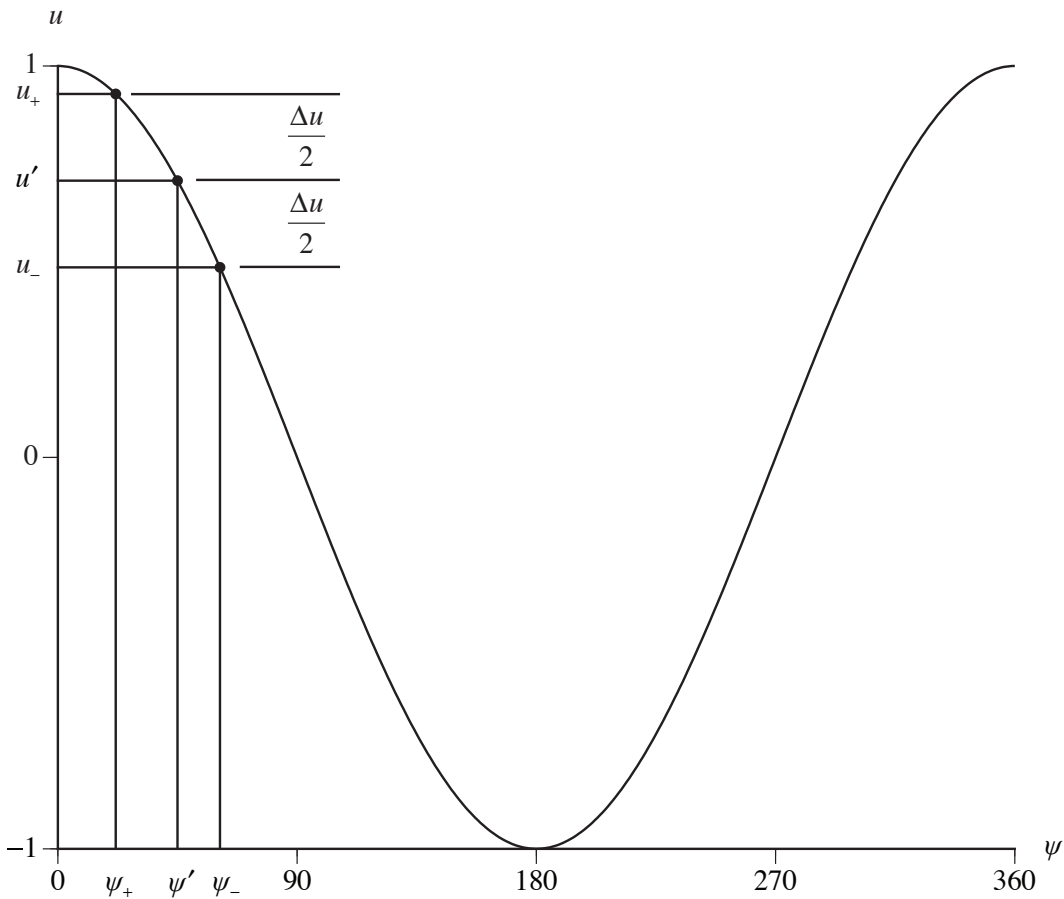


Figure 2.5-2 Direction cosine u versus bearing angle ψ (in deg) where $u = \cos \psi$ in the XY plane.

$$\cos^{-1}(x) = \frac{\pi}{2} - \sin^{-1}(x), \quad (2.5-13)$$

$$\cos^{-1}(-x) = \frac{\pi}{2} + \sin^{-1}(x), \quad (2.5-14)$$

and as a result,

$$\cos^{-1}(-x) - \cos^{-1}(x) = 2 \sin^{-1}(x). \quad (2.5-15)$$

Also note that $\psi' = 0^\circ$ and $\psi' = 180^\circ$ corresponds to steering the horizontal beam pattern to end-fire. However, (2.5-12) is *invalid* for $\psi' = 0^\circ$ and $\psi' = 180^\circ$. Therefore, a different approach must be used in order to compute the beamwidth at end-fire.

Beamwidth at End-Fire

Restricting ourselves once again to the horizontal, far-field beam pattern of a linear aperture lying along the X axis, consider the case where the beam-steer angle $\psi' = 0^\circ$ in the XY plane (see Fig. 2.5-1). With $\psi' = 0^\circ$, $u' = 1$ [see (2.5-3)], and as a result, (2.5-6) becomes (see Fig. 2.5-3)

$$u_- = 1 - \frac{\Delta u}{2}. \quad (2.5-16)$$

Also, with $\psi' = 0^\circ$, the half-beamwidth angle $\psi_- - \psi'$ reduces to ψ_- where

$$\psi_- = \Delta\psi/2 \quad (2.5-17)$$

since $\cos\psi$ is symmetric about $\psi = \psi' = 0^\circ$ (see Fig. 2.5-2). Therefore, substituting (2.5-17) into (2.5-2) yields

$$u_- = \cos(\Delta\psi/2), \quad (2.5-18)$$

and by equating the right-hand sides of (2.5-16) and (2.5-18), we finally obtain

$$\Delta\psi = 2 \cos^{-1} \left(1 - \frac{\Delta u}{2} \right), \quad \left| 1 - \frac{\Delta u}{2} \right| \leq 1$$

(2.5-19)

where $\Delta\psi$ is the 3-dB beamwidth in degrees of a horizontal, far-field beam pattern in the XY plane steered to end-fire (see Table 2.3-1 for Δu).

Let us end our discussion in this section by illustrating the distortion a beam pattern undergoes due to beam steering. By referring to (2.2-11), the normalized, far-field beam pattern of the rectangular amplitude window steered to $u = u'$ is given by

$$D_N(f, u - u') = \text{sinc} \left[\frac{L}{\lambda} (u - u') \right]. \quad (2.5-20)$$

The corresponding normalized, *horizontal*, far-field beam pattern is given by

$$D_N(f, 90^\circ, \psi) = \text{sinc} \left[\frac{L}{\lambda} (\cos\psi - \cos\psi') \right], \quad \theta' = 90^\circ. \quad (2.5-21)$$

Polar plots of the magnitude of (2.5-21) versus ψ for $L/\lambda = 4$ and for different

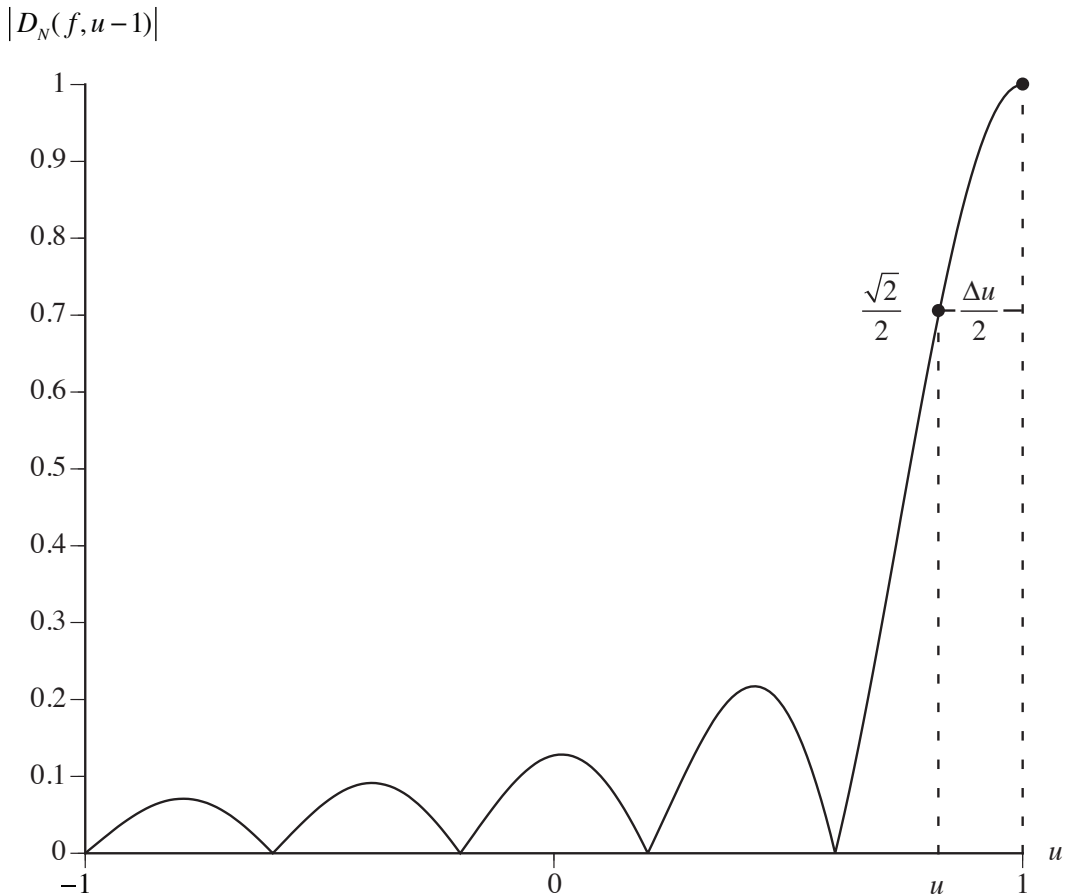


Figure 2.5-3 Magnitude of a typical normalized, far-field beam pattern of a linear aperture lying along the X axis, steered in the direction $u' = 1$ (end-fire).

values of ψ' are shown in Fig. 2.5-4. Note how *the beamwidth increases and the mainlobe becomes more asymmetrical about the beam-steer axis* as the beam pattern is steered from broadside ($\psi' = 90^\circ$) to end-fire ($\psi' = 0^\circ$).

Figure 2.5-4 also illustrates the *port/starboard (left/right) ambiguity problem* associated with linear apertures (linear arrays). For example, if the linear aperture is being used in the passive mode as a receiver trying to estimate the bearing angle to a sound-source (target), by referring to Fig. 2.5-4 (d), a sound-source at bearing angle $\psi = 45^\circ$ or $\psi = 315^\circ$ will produce the same output electrical signal from the linear aperture. Solutions to the port/starboard (left/right) ambiguity problem are discussed in Chapters 8 and 9, Examples 8.2-1 and 9.1-2, respectively.

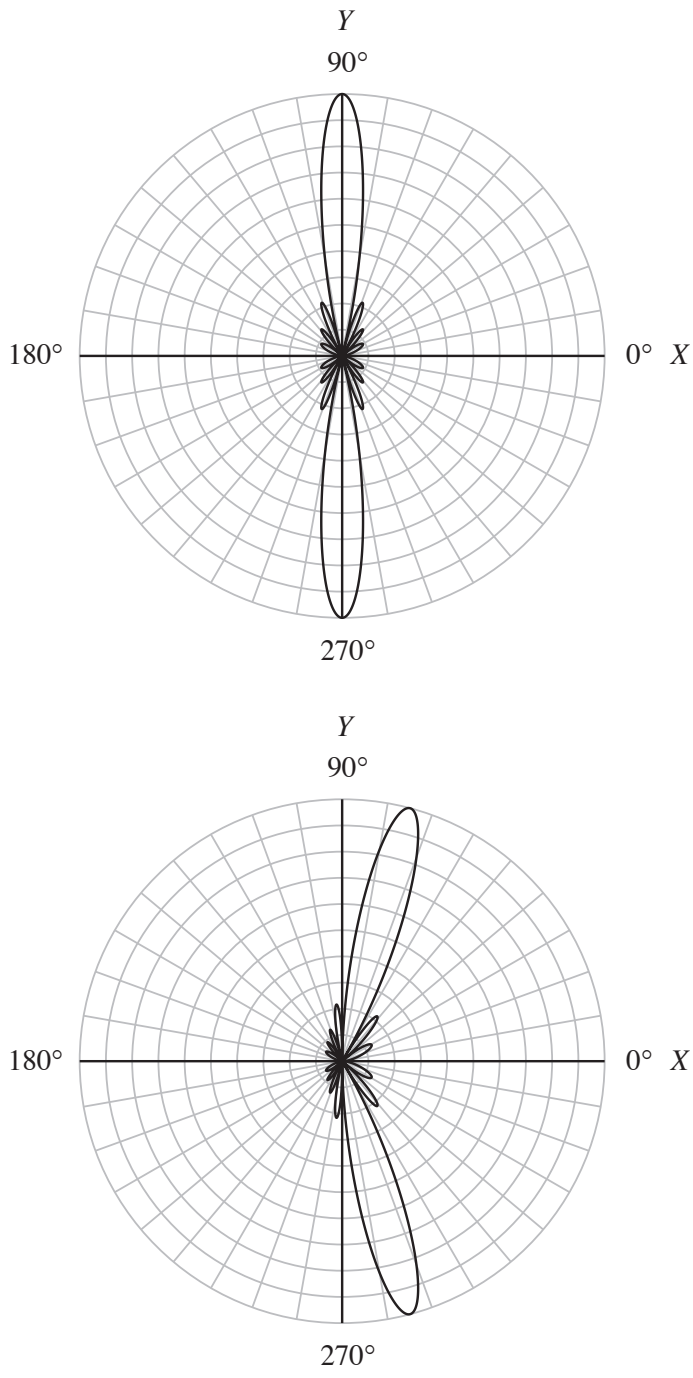
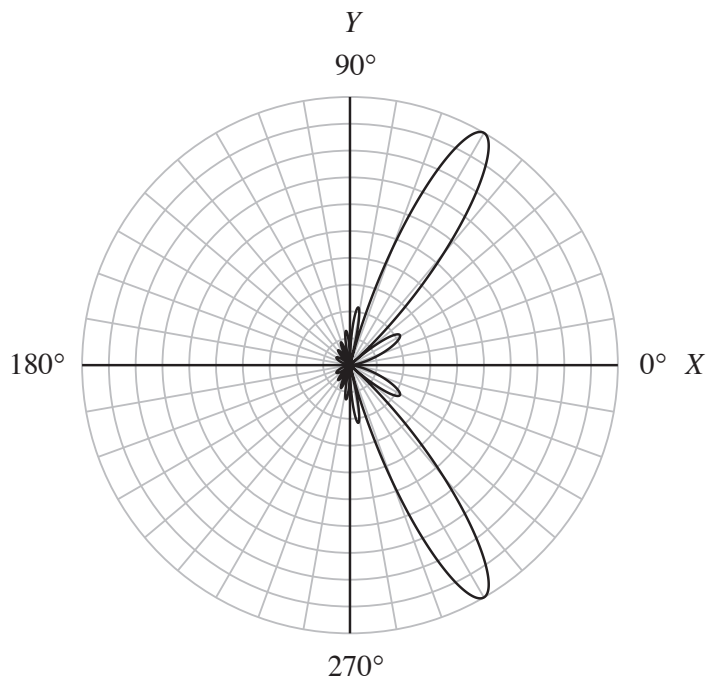
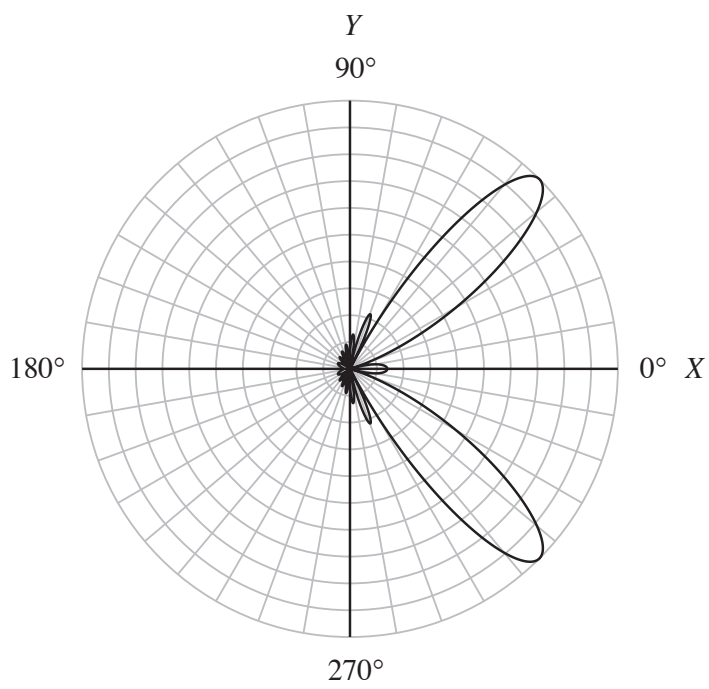


Figure 2.5-4 Polar plots, as a function of the azimuthal (bearing) angle ψ , of the magnitude of the normalized, horizontal, far-field beam pattern of the rectangular amplitude window given by (2.5-21) for $L/\lambda = 4$ and for beam-steer angle (a) $\psi' = 90^\circ$ (broadside), (b) $\psi' = 75^\circ$, (c) $\psi' = 60^\circ$, (d) $\psi' = 45^\circ$, (e) $\psi' = 30^\circ$, and (f) $\psi' = 0^\circ$ (end-fire).

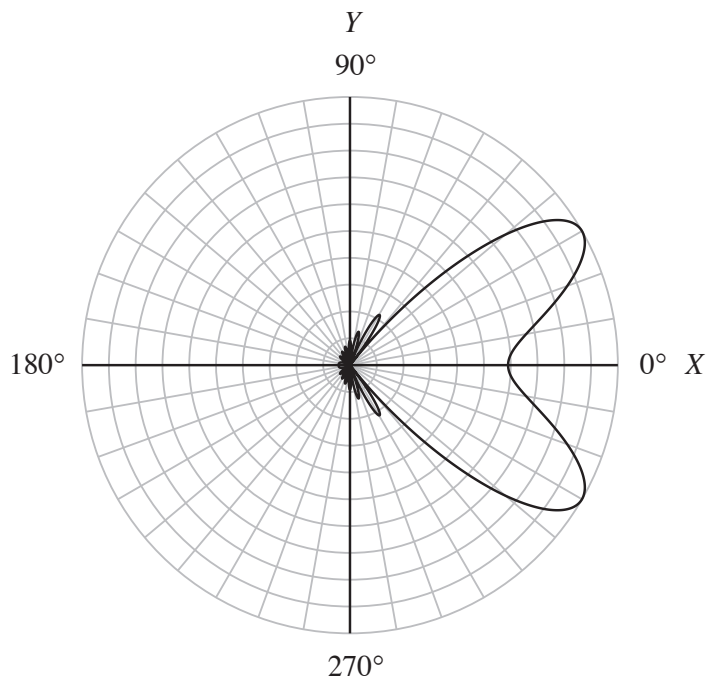


(c)

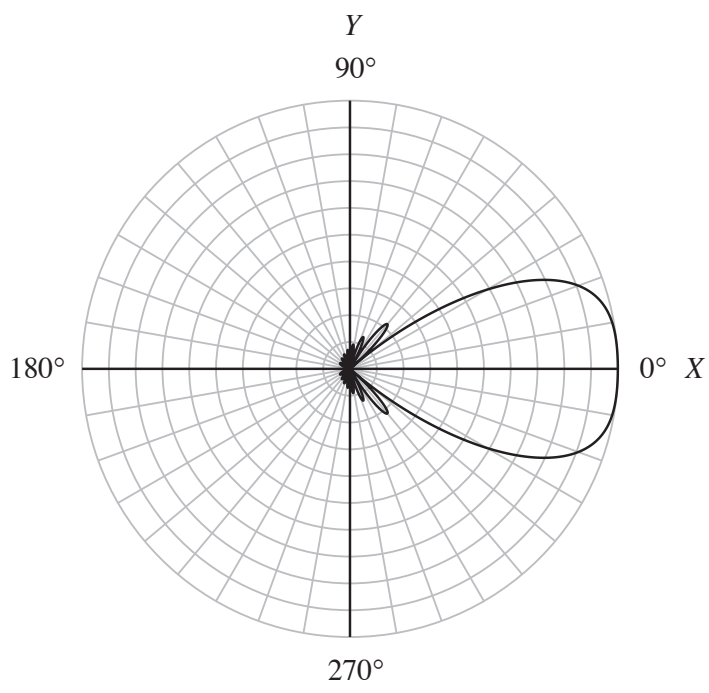


(d)

Figure 2.5-4 continued.



(e)



(f)

Figure 2.5-4 continued.

2.6 The Near-Field Beam Pattern of a Linear Aperture

In this section we shall demonstrate that the near-field beam pattern of a linear aperture is just a special case of the near-field beam pattern of a volume aperture. In [Section 1.2](#) it was shown that the near-field beam pattern (directivity function) of a closed-surface, volume aperture – based on the Fresnel approximation of a time-independent, free-space, Green's function – is given by the following three-dimensional spatial Fresnel transform:

$$\begin{aligned}\mathcal{D}(f, r, \alpha) &= F_{\mathbf{r}_A} \left\{ A(f, \mathbf{r}_A) \exp\left(-j \frac{k}{2r} r_A^2\right) \right\} \\ &= \int_{-\infty}^{\infty} A(f, \mathbf{r}_A) \exp\left(-j \frac{k}{2r} r_A^2\right) \exp(+j2\pi\alpha \cdot \mathbf{r}_A) d\mathbf{r}_A,\end{aligned}\quad (2.6-1)$$

where

$$\mathbf{r}_A = (x_A, y_A, z_A), \quad (2.6-2)$$

$$k = 2\pi f/c = 2\pi/\lambda, \quad (2.6-3)$$

$$r_A^2 = |\mathbf{r}_A|^2 = x_A^2 + y_A^2 + z_A^2, \quad (2.6-4)$$

$$r = |\mathbf{r}| = \sqrt{x^2 + y^2 + z^2}, \quad (2.6-5)$$

$$\alpha = (f_X, f_Y, f_Z), \quad (2.6-6)$$

$$\alpha \cdot \mathbf{r}_A = f_X x_A + f_Y y_A + f_Z z_A, \quad (2.6-7)$$

$$d\mathbf{r}_A = dx_A dy_A dz_A, \quad (2.6-8)$$

and $F_{\mathbf{r}_A}\{\cdot\}$ is shorthand notation for $F_{x_A} F_{y_A} F_{z_A}\{\cdot\}$. The complex aperture function $A(f, \mathbf{r}_A)$ can be expressed as

$$A(f, \mathbf{r}_A) = a(f, \mathbf{r}_A) \exp[+j\theta(f, \mathbf{r}_A)], \quad (2.6-9)$$

where $a(f, \mathbf{r}_A)$ is the *amplitude response* and $\theta(f, \mathbf{r}_A)$ is the *phase response* of the aperture at \mathbf{r}_A . Both $a(f, \mathbf{r}_A)$ and $\theta(f, \mathbf{r}_A)$ are *real* functions. The function $a(f, \mathbf{r}_A)$ is also known as the *amplitude window*. The units of $a(f, \mathbf{r}_A)$ and, hence, $A(f, \mathbf{r}_A)$ depend on whether the aperture is a transmit aperture (see [Table 1B-1](#) in [Appendix 1B](#)) or a receive aperture (see [Table 1B-2](#) in [Appendix 1B](#)).

The units of $\theta(f, \mathbf{r}_A)$ are radians.

Now consider the case of a *linear aperture* of length L meters lying along the X axis as shown in Fig. 2.1-1. As was mentioned earlier, a linear aperture can represent either a single electroacoustic transducer (e.g., a continuous line source or receiver) or a linear array of many individual electroacoustic transducers. Also shown in Fig. 2.1-1 is a field point with spherical coordinates (r, θ, ψ) . The field point is in the Fresnel region of the aperture, where the Fresnel angle criterion given by either (1.2-35) or (1.2-91) is satisfied, and the range r satisfies the Fresnel range criterion given by $1.356R_A < r < \pi R_A^2 / \lambda$ [see either (1.2-40) or (1.2-92)], where $R_A = L/2$ is the maximum radial extent of the linear aperture. Some typical values for the range to the near-field/far-field boundary $r_{\text{NF/FF}} = \pi R_A^2 / \lambda$ for three different frequencies f and two different lengths L for a *linear towed array* (an example of a linear aperture) are shown in Table 2.6-1, along with values for $r_{\min} = 1.356R_A$.

Table 2.6-1 Values for the Range to the Near-Field/Far-Field Boundary $r_{\text{NF/FF}}$ for a *Linear Towed Array* (an Example of a Linear Aperture)

c (m/sec)	f (Hz)	λ (m)	L (m)	R_A (m)	r_{\min} (m)	$r_{\text{NF/FF}}$ (km)
1500	60	25.0	100	50	67.8	0.314
1500	100	15.0	100	50	67.8	0.524
1500	1000	1.5	100	50	67.8	5.236
<hr/>						
1500	60	25.0	200	100	135.6	1.257
1500	100	15.0	200	100	135.6	2.094
1500	1000	1.5	200	100	135.6	20.944

Since the linear aperture in Fig. 2.1-1 is lying along the X axis, the position vector to a point on the surface of the aperture is given by

$$\mathbf{r}_A = (x_A, 0, 0), \quad (2.6-10)$$

and as a result,

$$A(f, \mathbf{r}_A) = A(f, x_A, y_A, z_A) \rightarrow A(f, x_A) \delta(y_A) \delta(z_A). \quad (2.6-11)$$

Therefore, by substituting (2.6-11) into (2.6-1) and using the sifting property of impulse functions, we obtain the following one-dimensional spatial Fresnel transform for the near-field beam pattern of a linear aperture lying along the X

axis:

$$\begin{aligned}\mathcal{D}(f, r, f_x) &= F_{x_A} \left\{ A(f, x_A) \exp\left(-j \frac{k}{2r} x_A^2\right) \right\} \\ &= \int_{-L/2}^{L/2} A(f, x_A) \exp\left(-j \frac{k}{2r} x_A^2\right) \exp(+j2\pi f_x x_A) dx_A\end{aligned}\quad (2.6-12)$$

where

$$A(f, x_A) = a(f, x_A) \exp[+j\theta(f, x_A)] \quad (2.6-13)$$

is the complex frequency response (complex aperture function) of the linear aperture,

$$k = 2\pi f/c = 2\pi/\lambda \quad (2.6-14)$$

is the wavenumber in radians per meter, and

$$f_x = u/\lambda = \sin\theta \cos\psi/\lambda \quad (2.6-15)$$

is a spatial frequency in the X direction with units of cycles per meter [see (1.2-43)]. Since f_x can be expressed in terms of the spherical angles θ and ψ , the near-field beam pattern can ultimately be expressed as a function of frequency f , the range r to a field point, and the spherical angles θ and ψ , that is, $\mathcal{D}(f, r, f_x) \rightarrow \mathcal{D}(f, r, \theta, \psi)$. If the linear aperture is a transmit aperture, then the aperture function $A(f, x_A)$ has units of $(m^3/sec)/V$ and the near-field beam pattern $\mathcal{D}(f, r, f_x)$ has units of $(m^3/sec)/V$. However, if the linear aperture is a receive aperture, then $A(f, x_A)$ has units of $(V/(m^2/sec))/m$ and $\mathcal{D}(f, r, f_x)$ has units of $V/(m^2/sec)$. These units are summarized in [Table 2.6-2](#). Equations (2.6-1) and (2.6-12) are most accurate in the Fresnel region of an aperture where both the Fresnel angle criterion and the Fresnel range criterion are satisfied. They are less accurate in the near-field region outside the Fresnel region where $r < r_{\text{NF/FF}}$, but the Fresnel angle criterion is *not* satisfied. As was discussed in [Subsection 1.2.1](#), the Fresnel region is only a subset of the near-field.

Finally, if a linear aperture lies along either the Y or Z axis instead of the X axis, then simply replace x_A and f_x with either y_A and f_y , or z_A and f_z , respectively, in (2.6-12), where spatial frequencies f_y and f_z are given by (1.2-44) and (1.2-45), respectively.

Table 2.6-2 Units of the Complex Aperture Function $A(f, x_A)$ and Corresponding Near-Field Beam Pattern $\mathcal{D}(f, r, f_X)$ for a Linear Aperture

Linear Aperture	$A(f, x_A)$	$\mathcal{D}(f, r, f_X)$
transmit	$(m^3/sec)/V$	$(m^3/sec)/V$
receive	$V/(m^2/sec)$	$V/(m^2/sec)$

2.6.1 Aperture Focusing

In order to discuss the concept of *aperture focusing*, let us investigate what happens to the near-field beam pattern given by (2.6-12) when the phase response $\theta(f, x_A)$ along the length of the aperture is a quadratic function of x_A , that is [see (2.4-1)],

$$\theta(f, x_A) = \theta_2(f)x_A^2, \quad (2.6-16)$$

where

$$\theta_2(f) = \frac{k}{2r'}, \quad (2.6-17)$$

and

$$k = 2\pi f/c = 2\pi/\lambda. \quad (2.6-18)$$

The quadratic phase response given by (2.6-16) is an *even* function of x_A and is a *parabola* that passes through the origin. The parameter r' in (2.6-17) is referred to as the *focal range*. It is the near-field range from the aperture where the far-field beam pattern of the aperture will be in focus. If (2.6-13), (2.6-16), and (2.6-17) are substituted into (2.6-12), then

$$\mathcal{D}(f, r, f_X) = \int_{-L/2}^{L/2} a(f, x_A) \exp\left[-j\frac{k}{2}\left(\frac{1}{r} - \frac{1}{r'}\right)x_A^2\right] \exp(+j2\pi f_X x_A) dx_A, \quad (2.6-19)$$

and if (2.6-19) is evaluated at the near-field range $r = r'$, then it reduces to

$$\mathcal{D}(f, r', f_X) = \int_{-L/2}^{L/2} a(f, x_A) \exp(+j2\pi f_X x_A) dx_A, \quad (2.6-20)$$

or

$$\mathcal{D}(f, r', f_X) = F_{x_A}\{a(f, x_A)\} = D(f, f_X), \quad (2.6-21)$$

where $D(f, f_x)$ is the *far-field* beam pattern of the amplitude response (amplitude window) $a(f, x_A)$. Therefore, (2.6-21) indicates that the far-field beam pattern of the amplitude window can be *focused* at the near-field range $r = r'$ meters from the aperture if the phase response $\theta(f, x_A)$ along the length of the aperture is given by (2.6-16) through (2.6-18). The quadratic phase response accurately compensates for wavefront curvature in the Fresnel region of the aperture. The physical situation represented by (2.6-21) is known as *aperture focusing*. However, in the near-field region of the aperture outside the Fresnel region, a quadratic phase response can only approximately focus the far-field beam pattern.

A good way to think about aperture focusing is to compare it with taking a photograph. If the subject is far enough away (in the far-field), we do not concern ourselves with the actual range to the subject – we simply set the focus on the camera to infinity and take the picture. However, if the subject is nearby (in the near-field), we do concern ourselves with the actual range to the subject since we must refocus the camera whenever the subject moves.

2.6.2 Beam Steering and Aperture Focusing

Let us investigate what happens to the near-field beam pattern given by (2.6-12) when the phase response $\theta(f, x_A)$ along the length of the aperture is equal to the sum of a linear and quadratic function of x_A , that is [see (2.4-1)],

$$\theta(f, x_A) = \theta_1(f)x_A + \theta_2(f)x_A^2, \quad (2.6-22)$$

where

$$\theta_1(f) = -2\pi f'_X, \quad (2.6-23)$$

$$\theta_2(f) = \frac{k}{2r'}, \quad (2.6-24)$$

$$f'_X = u'/\lambda = \sin\theta' \cos\psi'/\lambda, \quad (2.6-25)$$

and

$$k = 2\pi f/c = 2\pi/\lambda. \quad (2.6-26)$$

If (2.6-13) and (2.6-22) through (2.6-24) are substituted into (2.6-12), then

$$\mathcal{D}(f, r, f_X) = \int_{-L/2}^{L/2} a(f, x_A) \exp\left[-j\frac{k}{2}\left(\frac{1}{r} - \frac{1}{r'}\right)x_A^2\right] \exp[j2\pi(f_X - f'_X)x_A] dx_A, \quad (2.6-27)$$

and if (2.6-27) is evaluated at the near-field range $r = r'$, then it reduces to

$$\mathcal{D}(f, r', f_X) = \int_{-L/2}^{L/2} a(f, x_A) \exp[j2\pi(f_X - f'_X)x_A] dx_A, \quad (2.6-28)$$

or

$$\mathcal{D}(f, r', f_X) = F_{x_A} \{a(f, x_A) \exp(-j2\pi f'_X x_A)\} = D(f, f_X - f'_X). \quad (2.6-29)$$

Equation (2.6-29) indicates that the far-field beam pattern $D(f, f_X)$ of the amplitude response (amplitude window) $a(f, x_A)$ is *in focus* at the near-field range $r = r'$ meters from the aperture, and has been *steered* in the direction $u = u'$ in direction-cosine space, which is equivalent to steering (tilting) the beam pattern to $\theta = \theta'$ and $\psi = \psi'$ [see (2.6-25)].

Problems

Section 2.2

- 2-1 Show that (2.2-4) is equal to (2.2-5).
- 2-2 Verify (2.2-9).
- 2-3 Derive the *normalized*, far-field beam patterns of the following aperture functions, expressing your answers in terms of the spherical angles θ and ψ :
- (a) $A(f, y_A) = A_A \text{rect}(y_A/L)$
 - (b) $A(f, z_A) = A_A \text{rect}(z_A/L)$
- 2-4 The aperture function of a linear aperture lying along the X axis is given by

$$A(f, x_A) = a(f, x_A) = \begin{cases} -A_A, & -L/2 \leq x_A < 0 \\ A_A, & 0 \leq x_A \leq L/2. \end{cases}$$

Find the unnormalized, far-field beam pattern of the aperture. This amplitude response is an example of an *odd* function of x_A .

- 2-5 Derive (2.2-20) by evaluating the spatial-domain, Fourier integral.
- 2-6 Show that

$$F_{f_X}^{-1}\{\delta(f_X \pm f'_X)\} = \exp(\pm j2\pi f'_X x_A).$$

From this result we can write that [see (2.2-26)]

$$F_{x_A}\{\exp(\pm j2\pi f'_X x_A)\} = \delta(f_X \pm f'_X),$$

and if $f'_X = 0$, then $F_{x_A}\{1\} = \delta(f_X)$ and $F_{f_X}^{-1}\{\delta(f_X)\} = 1$.

- 2-7 Show that

$$g(x) * \delta(x \pm x_0) = g(x \pm x_0),$$

where the asterisk denotes convolution with respect to x , and x_0 is an arbitrary constant.

- 2-8 The complex frequency response (complex aperture function) of a linear aperture lying along the Y axis is modeled by the cosine amplitude window. Evaluate the *normalized*, far-field beam pattern of the aperture at $\theta = 40^\circ$ and $\psi = 108^\circ$. Use $L/\lambda = 2$.
- 2-9 If the aperture function of a linear aperture lying along the X axis is modeled by the *sine* amplitude window, that is, if

$$A(f, x_A) = a(f, x_A) = A_A \sin(\pi x_A / L) \text{rect}(x_A / L),$$

then find the unnormalized, far-field beam pattern of the aperture. The sine amplitude window is an example of an *odd* function of x_A .

- 2-10 Derive the *normalized*, far-field beam patterns of the Hanning, Hamming, and Blackman amplitude windows. Use the following trigonometric identity: $\sin(\alpha \pm \pi) = -\sin \alpha$.

Section 2.2 Appendix 2A

- 2-11 Find the transmitter sensitivity functions for the following complex frequency responses of a continuous line source lying along the X axis where $A_A(f)$ is a real, nonnegative function of frequency:

- (a) rectangular amplitude window: $A_T(f, x_A) = A_A(f) \text{rect}(x_A / L)$
- (b) cosine amplitude window: $A_T(f, x_A) = A_A(f) \cos(\pi x_A / L) \text{rect}(x_A / L)$

- 2-12 If the transmitter sensitivity level (transmitting voltage response) of a continuous line source at 16 kHz is 140 dB re $1 \mu\text{Pa}/\text{V}$ at 1 m , then what is the value of the magnitude of the transmitter sensitivity function in $(\text{m}^3/\text{sec})/\text{V}$? Use $\rho_0 = 1026 \text{ kg/m}^3$ for the ambient density of seawater. The length L of the continuous line source is less than 0.632 m or 24.9 in .
- 2-13 If the receiver sensitivity level (open circuit receiving response) of a continuous line receiver at 2 kHz is $-195 \text{ dB re } 1 \text{ V}/\mu\text{Pa}$, then what is the value of the magnitude of the receiver sensitivity function in $\text{V}/(\text{m}^2/\text{sec})$? Use $\rho_0 = 1026 \text{ kg/m}^3$ for the ambient density of seawater.

Section 2.3

- 2-14 Compute the 3-dB beamwidths of the horizontal, far-field beam patterns of the rectangular, triangular, cosine, Hanning, Hamming, and Blackman amplitude windows for $L/\lambda = 0.5, 1, 2, \text{ and } 4$.
- 2-15 Consider a *linear towed array* (an example of a linear aperture) lying along the X axis. The amplitude response of the aperture is modeled by the rectangular amplitude window. How long must the aperture be in order for the 3-dB beamwidth of the horizontal, far-field beam pattern to be 10° at broadside for $f = 100 \text{ Hz}$? Use $c = 1500 \text{ m/sec}$.

Section 2.4

- 2-16 Consider a linear aperture lying along the X axis. If $f = 1 \text{ kHz}$ and $c = 1500 \text{ m/sec}$, then
- what must the phase response of the aperture be in order to steer the mainlobe of the aperture's far-field beam pattern to $\theta' = 49^\circ$ and $\psi' = 71^\circ$.
 - Repeat (a) for a linear aperture lying along the Y axis.
 - Repeat (a) for a linear aperture lying along the Z axis.

Section 2.5

- 2-17 Compute the 3-dB beamwidths of the horizontal, far-field beam patterns of the rectangular, triangular, cosine, Hanning, Hamming, and Blackman amplitude windows for the following beam-steer angles: $\psi' = 90^\circ$

(broadside), 75° , 60° , 45° , 30° , and 0° (end-fire). Use $L/\lambda = 4$.

- 2-18 The complex aperture function of a *linear towed array* (an example of a linear aperture) lying along the X axis is modeled by the rectangular amplitude window. The length of the aperture is 200 m. Using $f = 60$ Hz and $c = 1500$ m/sec, compute the 3-dB beamwidth of the horizontal, far-field beam pattern of this aperture at
- broadside
 - a beam-steer angle of 30°
 - Compute *both* half-beamwidth angles at a beam-steer angle of 30° .
 - Repeat (a) through (c) for $f = 100$ Hz.

- 2-19 Consider a linear aperture lying along the X axis.

- (a) Show that the 3-dB beamwidth of the vertical, far-field beam pattern in the XZ plane is given by

$$\Delta\theta = \sin^{-1}\left(\sin\theta' + \frac{\Delta u}{2}\right) - \sin^{-1}\left(\sin\theta' - \frac{\Delta u}{2}\right), \quad \left|\sin\theta' \pm \frac{\Delta u}{2}\right| \leq 1,$$

where θ' is the beam-steer angle in the XZ plane. Note that $\theta' = 0^\circ$ corresponds to an unsteered vertical beam pattern and, in this case, $\Delta\theta$ reduces to (2.3-19) since

$$\sin^{-1}(-x) = -\sin^{-1}(x).$$

Hint: follow a procedure analogous to the one used to derive (2.5-12).

- (b) Show that the 3-dB beamwidth of the vertical, far-field beam pattern in the XZ plane steered to end-fire is given by

$$\Delta\theta = 2\cos^{-1}\left(1 - \frac{\Delta u}{2}\right), \quad \left|1 - \frac{\Delta u}{2}\right| \leq 1.$$

Hint: follow a procedure analogous to the one used to derive (2.5-19).

Section 2.6

- 2-20 The spherical coordinates of a sound source (target) as measured from the

center of a *linear towed array* (an example of a linear aperture) lying along the X axis are $r_s = 4 \text{ km}$, $\theta_s = 100^\circ$, and $\psi_s = 75^\circ$. The length of the aperture is 100 m. If $f = 1 \text{ kHz}$ and $c = 1500 \text{ m/sec}$,

- (a) is the sound source in the aperture's Fresnel region or far-field?
- (b) What must the phase response along the length of the aperture be if the aperture's far-field beam pattern is to be focused (if required) and steered to coordinates (r_s, θ_s, ψ_s) ?
- (c) If the range to the sound source r_s and the vertical angle θ_s remain the same, but the bearing angle changes to $\psi_s = 65^\circ$, is the sound source in the aperture's Fresnel region or far-field?

Appendix 2A Transmitter and Receiver Sensitivity Functions of a Continuous Line Transducer

Transmitter Sensitivity Function

For the case of a continuous line source lying along the X axis, the complex, *transmitter sensitivity function* $S_T(f)$ is related to the complex, transmit frequency response $A_T(f, x_A)$ of the transducer as follows (see [Example 2B-1](#) in [Appendix 2B](#)):

$$S_T(f) = \int_{-\infty}^{\infty} A_T(f, x_A) dx_A \quad (2A-1)$$

where $S_T(f)$ has units of $(\text{m}^3/\text{sec})/\text{V}$ and $A_T(f, x_A)$ has units of $((\text{m}^3/\text{sec})/\text{V})/\text{m}$ (see [Table 2.1-1](#)). However, manufacturers of electroacoustic transducers usually describe the *transmitting voltage response* of a transducer by plotting the *transmitter sensitivity level* $TSL(f)$ in dB re TS_{ref} at 1 m versus frequency f in hertz. The notation “dB re TS_{ref} ” means decibels relative to a reference transmitter sensitivity. In underwater acoustics, the reference transmitter sensitivity TS_{ref} is usually $1 \mu\text{Pa}/\text{V}$. The corresponding *transmitter sensitivity* $TS(f)$ with units of Pa/V is given by

$$TS(f) = TS_{ref} 10^{[TSL(f)/20]} \quad (2A-2)$$

The transmitter sensitivity $TS(f)$ is a *real, nonnegative* function of frequency.

Values for the magnitude of the transmitter sensitivity function, $|\mathcal{S}_T(f)|$ in $(\text{m}^3/\text{sec})/\text{V}$, for a continuous line source of length L meters lying along the X axis and centered at the origin of the coordinate system as shown in Fig. 2.1-1, can be obtained from measured values of the transmitter sensitivity, $\text{TS}(f)$ in Pa/V , by using the following formula (see Example 2B-1 in Appendix 2B):

$$\boxed{|\mathcal{S}_T(f)| = \frac{2r}{f\rho_0} \text{TS}(f) \Big|_{r=1\text{ m}}, \quad L < 0.632 \text{ m}} \quad (2A-3)$$

where

$$r = \sqrt{y^2 + z^2} \quad (2A-4)$$

is the distance from the center of the continuous line source to a field point at *broadside* relative to the continuous line source, ρ_0 is the constant ambient (equilibrium) density of the fluid medium in kilograms per cubic meter, and $\text{TS}(f)$ is given by (2A-2). Note that (2A-3) is valid only if the length L of the continuous line source is less than 0.632 m or 24.9 in.

Receiver Sensitivity Function

For the case of a continuous line receiver lying along the X axis, the complex, *receiver sensitivity function* $\mathcal{S}_R(f)$ is related to the complex, receive frequency response $A_R(f, x_A)$ of the transducer as follows:

$$\boxed{\mathcal{S}_R(f) = \int_{-\infty}^{\infty} A_R(f, x_A) dx_A} \quad (2A-5)$$

where $\mathcal{S}_R(f)$ has units of $\text{V}/(\text{m}^2/\text{sec})$ and $A_R(f, x_A)$ has units of $(\text{V}/(\text{m}^2/\text{sec}))/\text{m}$ (see Table 2.1-1). However, manufacturers of electroacoustic transducers usually describe the *open circuit receiving response* of a transducer by plotting the *receiver sensitivity level* $\text{RSL}(f)$ in dB re RS_{ref} versus frequency f in hertz. The notation “dB re RS_{ref} ” means decibels relative to a reference receiver sensitivity. In underwater acoustics, the reference receiver sensitivity RS_{ref} is usually $1\text{V}/\mu\text{Pa}$. The corresponding *receiver sensitivity* $\text{RS}(f)$ with units of V/Pa is given by

$$\boxed{\text{RS}(f) = \text{RS}_{\text{ref}} 10^{[\text{RSL}(f)/20]}} \quad (2A-6)$$

The receiver sensitivity $\text{RS}(f)$ is a *real, nonnegative* function of frequency. What we need to do next is to derive the conversion factor that will allow us to convert m^2/sec to Pa for a time-harmonic acoustic field.

The derivation of the desired conversion factor in this case is simple. By computing the magnitude of (2B-24), we obtain

$$\left| p_f(\mathbf{r}) \right| = 2\pi f \rho_0 \left| \varphi_f(\mathbf{r}) \right|, \quad (2A-7)$$

from which we obtain the conversion factor

$$\boxed{\frac{\left| p_f(\mathbf{r}) \right|}{\left| \varphi_f(\mathbf{r}) \right|} = 2\pi f \rho_0 \frac{\text{Pa}}{\text{m}^2/\text{sec}}} \quad (2A-8)$$

where $p_f(\mathbf{r}) \equiv p_f(x, y, z)$ and $\varphi_f(\mathbf{r}) \equiv \varphi_f(x, y, z)$. The conversion factor on the right-hand-side of (2A-8) is used to convert velocity potential in m^2/sec to acoustic pressure in Pa for a time-harmonic acoustic field. Therefore, values for the magnitude of the receiver sensitivity function, $|\mathcal{S}_R(f)|$ in $\text{V}/(\text{m}^2/\text{sec})$, can be obtained from measured values of the receiver sensitivity, $\text{RS}(f)$ in V/Pa , by using the following formula:

$$\boxed{|\mathcal{S}_R(f)| = 2\pi f \rho_0 \text{RS}(f)} \quad (2A-9)$$

where ρ_0 is the constant ambient (equilibrium) density of the fluid medium in kilograms per cubic meter and $\text{RS}(f)$ is given by (2A-6).

Appendix 2B Radiation from a Linear Aperture

An exact solution of the linear wave equation given by (1.2-1) for free-space propagation in an ideal (nonviscous), homogeneous, fluid medium is given by [see (1.2-3)]

$$\varphi(t, \mathbf{r}) = \int_{-\infty}^{\infty} \int_{V_0} X(f, \mathbf{r}_0) A_T(f, \mathbf{r}_0) g_f(\mathbf{r} | \mathbf{r}_0) dV_0 \exp(+j2\pi ft) df, \quad (2B-1)$$

where $\varphi(t, \mathbf{r})$ is the scalar velocity potential in squared meters per second,

$X(f, \mathbf{r}_0)$ is the complex frequency spectrum of the input electrical signal at location \mathbf{r}_0 of the transmit aperture with units of volts per hertz, $A_T(f, \mathbf{r}_0)$ is the complex frequency response of the transmit aperture at \mathbf{r}_0 with units of $((\text{m}^3/\text{sec})/\text{V})/\text{m}^3$,

$$g_f(\mathbf{r} | \mathbf{r}_0) = -\frac{\exp(-jk|\mathbf{r} - \mathbf{r}_0|)}{4\pi|\mathbf{r} - \mathbf{r}_0|} = -\frac{\exp(-jkR)}{4\pi R} \quad (2B-2)$$

is the time-independent, free-space, Green's function of an unbounded, ideal (nonviscous), homogeneous, fluid medium with units of inverse meters,

$$k = 2\pi f/c = 2\pi/\lambda \quad (2B-3)$$

is the wavenumber in radians per meter, $c = f\lambda$ is the constant speed of sound in the fluid medium in meters per second, λ is the wavelength in meters,

$$\mathbf{r} = x\hat{x} + y\hat{y} + z\hat{z} \quad (2B-4)$$

is the position vector to a field point,

$$\mathbf{r}_0 = x_0\hat{x} + y_0\hat{y} + z_0\hat{z} \quad (2B-5)$$

is the position vector to a source point, and

$$R = |\mathbf{r} - \mathbf{r}_0| = \sqrt{(x - x_0)^2 + (y - y_0)^2 + (z - z_0)^2} \quad (2B-6)$$

is the range in meters between a source point and a field point. If an identical input electrical signal is applied at all locations \mathbf{r}_0 of the transmit aperture, then (see [Example 1.2-1](#))

$$x(t, \mathbf{r}_0) = x(t) \quad (2B-7)$$

and

$$X(f, \mathbf{r}_0) = X(f), \quad (2B-8)$$

where $X(f)$ is the complex frequency spectrum of $x(t)$. Substituting (2B-8) into (2B-1) yields

$$\varphi(t, \mathbf{r}) = \int_{-\infty}^{\infty} X(f) \int_{V_0} A_T(f, \mathbf{r}_0) g_f(\mathbf{r} | \mathbf{r}_0) dV_0 \exp(+j2\pi ft) df. \quad (2B-9)$$

For the case of a linear aperture lying along the X axis,

$$\mathbf{r}_0 = (x_0, 0, 0), \quad (2B-10)$$

and as a result,

$$A_T(f, \mathbf{r}_0) = A_T(f, x_0, y_0, z_0) \rightarrow A_T(f, x_0) \delta(y_0) \delta(z_0). \quad (2B-11)$$

Substituting (2B-11) into (2B-9) yields

$$\varphi(t, \mathbf{r}) = \int_{-\infty}^{\infty} X(f) \int_{-\infty}^{\infty} A_T(f, x_0) g_f(\mathbf{r} | \mathbf{r}_0) dx_0 \exp(+j2\pi ft) df \quad (2B-12)$$

where $g_f(\mathbf{r} | \mathbf{r}_0)$ is given by (2B-2) and

$$R = |\mathbf{r} - \mathbf{r}_0| = \sqrt{(x - x_0)^2 + y^2 + z^2}. \quad (2B-13)$$

Equation (2B-12) is a general expression for the scalar velocity potential of the acoustic field radiated by a linear aperture lying along the X axis. The corresponding solution for the radiated acoustic pressure $p(t, \mathbf{r})$ in pascals can be obtained by substituting (2B-12) into (1.2-8). Doing so yields

$$p(t, \mathbf{r}) = -j2\pi\rho_0 \int_{-\infty}^{\infty} f X(f) \int_{-\infty}^{\infty} A_T(f, x_0) g_f(\mathbf{r} | \mathbf{r}_0) dx_0 \exp(+j2\pi ft) df \quad (2B-14)$$

where ρ_0 is the constant ambient (equilibrium) density of the fluid medium in kilograms per cubic meter, and $g_f(\mathbf{r} | \mathbf{r}_0)$ is given by (2B-2) and (2B-13).

If the input electrical signal is time-harmonic, that is, if (see [Example 1.2-1](#))

$$x(t) = A_x \exp(+j2\pi f_0 t), \quad (2B-15)$$

where A_x is the complex amplitude with units of volts, then

$$X(f) = A_x \delta(f - f_0), \quad (2B-16)$$

where the impulse function $\delta(f - f_0)$ has units of inverse hertz. Substituting (2B-16) into (2B-12) yields

$$\varphi(t, \mathbf{r}) = A_x \int_{-\infty}^{\infty} A_T(f_0, x_0) g_{f_0}(\mathbf{r} | \mathbf{r}_0) dx_0 \exp(+j2\pi f_0 t), \quad (2B-17)$$

and by replacing f_0 with f ,

$$\boxed{\varphi(t, \mathbf{r}) = A_x \int_{-\infty}^{\infty} A_T(f, x_0) g_f(\mathbf{r} | \mathbf{r}_0) dx_0 \exp(+j2\pi ft)} \quad (2B-18)$$

or

$$\varphi(t, \mathbf{r}) = \varphi_f(\mathbf{r}) \exp(+j2\pi ft), \quad (2B-19)$$

where

$$\varphi_f(\mathbf{r}) = A_x \int_{-\infty}^{\infty} A_T(f, x_0) g_f(\mathbf{r} | \mathbf{r}_0) dx_0 \quad (2B-20)$$

and $g_f(\mathbf{r} | \mathbf{r}_0)$ is given by (2B-2) and (2B-13). Equation (2B-18) is the time-harmonic, scalar velocity potential of the acoustic field radiated by a linear aperture lying along the X axis. The corresponding solution for the time-harmonic, radiated acoustic pressure $p(t, \mathbf{r})$ in pascals is given by

$$\boxed{p(t, \mathbf{r}) = -j2\pi f \rho_0 A_x \int_{-\infty}^{\infty} A_T(f, x_0) g_f(\mathbf{r} | \mathbf{r}_0) dx_0 \exp(+j2\pi ft)} \quad (2B-21)$$

or

$$p(t, \mathbf{r}) = p_f(\mathbf{r}) \exp(+j2\pi ft), \quad (2B-22)$$

where

$$p_f(\mathbf{r}) = -j2\pi f \rho_0 A_x \int_{-\infty}^{\infty} A_T(f, x_0) g_f(\mathbf{r} | \mathbf{r}_0) dx_0 \quad (2B-23)$$

and $g_f(\mathbf{r} | \mathbf{r}_0)$ is given by (2B-2) and (2B-13). Note that

$$p_f(\mathbf{r}) = -j2\pi f \rho_0 \varphi_f(\mathbf{r}), \quad (2B-24)$$

where $\varphi_f(\mathbf{r})$ is given by (2B-20).

Example 2B-1 Transmitter Sensitivity Function and Source Strength of a Continuous Line Source

Consider the case of a continuous line source (an example of a linear aperture) lying along the X axis and centered at the origin of the coordinate system as shown in Fig. 2.1-1. The transducer is L meters in length and extends from $-L/2$ to $L/2$ along the X axis. Therefore,

$$\int_{-\infty}^{\infty} A_T(f, x_0) g_f(\mathbf{r} | \mathbf{r}_0) dx_0 = \int_{-L/2}^{L/2} A_T(f, x_0) g_f(\mathbf{r} | \mathbf{r}_0) dx_0 , \quad (2B-25)$$

where $g_f(\mathbf{r} | \mathbf{r}_0)$ is given by (2B-2) and (2B-13). If the radiated acoustic field is measured at *broadsides* at $\mathbf{r} = (0, y, z)$, then (2B-13) reduces to

$$R = |\mathbf{r} - \mathbf{r}_0| = r \sqrt{1 + (x_0/r)^2} , \quad (2B-26)$$

where

$$r = \sqrt{y^2 + z^2} \quad (2B-27)$$

is the range in meters to a field point. Note that $r \neq 0$. Setting x_0 equal to either the upper or lower limit of integration $\pm L/2$ in (2B-26) yields

$$R = |\mathbf{r} - \mathbf{r}_0| = r \sqrt{1 + \left(\frac{L}{2r}\right)^2} , \quad (2B-28)$$

and if

$$\left(\frac{L}{2r}\right)^2 < 0.1 , \quad (2B-29)$$

or

$$L < 0.632 r , \quad (2B-30)$$

then

$$R = |\mathbf{r} - \mathbf{r}_0| \approx r , \quad L < 0.632 r , \quad (2B-31)$$

for $\mathbf{r} = (0, y, z)$ and $\mathbf{r}_0 = (x_0, 0, 0)$, where $|x_0| \leq L/2$. Therefore, substituting (2B-31) into (2B-2) yields

$$g_f(\mathbf{r} | \mathbf{r}_0) = g_f(0, y, z | x_0, 0, 0) \approx -\frac{\exp(-jkr)}{4\pi r} , \quad L < 0.632 r , \quad (2B-32)$$

and substituting (2B-32) into (2B-25) yields

$$\int_{-\infty}^{\infty} A_T(f, x_0) g_f(\mathbf{r} | \mathbf{r}_0) dx_0 \approx -\frac{\exp(-jkr)}{4\pi r} \mathcal{S}_T(f) , \quad L < 0.632 r , \quad (2B-33)$$

where

$$\boxed{\mathcal{S}_T(f) = \int_{-L/2}^{L/2} A_T(f, x_0) dx_0} \quad (2B-34)$$

is the *transmitter sensitivity function* in $(\text{m}^3/\text{sec})/\text{V}$. Next we shall use (2B-33) to compute the time-harmonic, radiated acoustic pressure at $\mathbf{r} = (0, y, z)$.

The time-harmonic, radiated acoustic pressure at $\mathbf{r} = (0, y, z)$ is given by

$$p(t, 0, y, z) = p_f(0, y, z) \exp(+j2\pi ft), \quad (2B-35)$$

where, by substituting (2B-33) into (2B-23),

$$p_f(0, y, z) \approx j \frac{f\rho_0}{2r} A_x \mathcal{S}_T(f) \exp(-jkr), \quad L < 0.632r, \quad (2B-36)$$

or

$$p_f(0, y, z) \approx j \frac{f\rho_0}{2r} S_0 \exp(-jkr), \quad L < 0.632r, \quad (2B-37)$$

where

$$\boxed{S_0 = A_x \mathcal{S}_T(f)} \quad (2B-38)$$

is the source strength of the continuous line source in cubic meters per second at frequency f hertz.

From (2B-35) it can be seen that

$$|p(t, 0, y, z)| = |p_f(0, y, z)|, \quad (2B-39)$$

where from (2B-36)

$$|p_f(0, y, z)| \approx \frac{f\rho_0}{2r} |A_x| |\mathcal{S}_T(f)|, \quad L < 0.632r. \quad (2B-40)$$

Therefore, using (2B-40) to solve for $|\mathcal{S}_T(f)|$ yields

$$\boxed{|\mathcal{S}_T(f)| \approx \frac{2r}{f\rho_0} \text{TS}(f), \quad L < 0.632r} \quad (2B-41)$$

where

$$\boxed{\text{TS}(f) = |p_f(0, y, z)| / |A_x|} \quad (2B-42)$$

is the *transmitter sensitivity* in pascals per volt, and r is the range to a field point with coordinates $(0, y, z)$ and is given by (2B-27). Recall that the range r is the distance from the center of the continuous line source to a field point at *broadside* relative to the continuous line source. Evaluating (2B-41) at $r = 1$ m yields

$$\left| \mathcal{S}_T(f) \right| \approx \frac{2r}{f\rho_0} \text{TS}(f) \Bigg|_{r=1\text{ m}}, \quad L < 0.632 \text{ m} \quad (2B-43)$$

Note that (2B-43) is valid only if the length L of the continuous line source is less than 0.632 m or 24.9 in.

The magnitude of the source strength can be obtained from (2B-37) as follows:

$$\left| S_0 \right| \approx \frac{2r}{f\rho_0} \left| p_f(0, y, z) \right|, \quad L < 0.632r \quad (2B-44)$$

where r is the range to a field point with coordinates $(0, y, z)$ and is given by (2B-27). Evaluating (2B-44) at $r = 1$ m yields

$$\left| S_0 \right| \approx \frac{2r}{f\rho_0} \left| p_f(0, y, z) \right| \Bigg|_{r=1\text{ m}}, \quad L < 0.632 \text{ m} \quad (2B-45)$$

Note that (2B-45) is valid only if the length L of the continuous line source is less than 0.632 m or 24.9 in. Also, from (2B-38),

$$\left| S_0 \right| = \left| A_x \right| \left| \mathcal{S}_T(f) \right| \quad (2B-46)$$

where the transmitter sensitivity function $\mathcal{S}_T(f)$ is given by (2B-34). ■

Appendix 2C Symmetry Properties and Far-Field Beam Patterns

The far-field beam pattern of a linear aperture lying along the X axis is given by [see (2.1-9)]

$$D(f, f_X) = \int_{-L/2}^{L/2} A(f, x_A) \exp(+j2\pi f_X x_A) dx_A, \quad (2C-1)$$

where

$$A(f, x_A) = a(f, x_A) \exp[+j\theta(f, x_A)] \quad (2C-2)$$

is the complex frequency response (complex aperture function) of the linear aperture [see (2.1-10)]. If the phase response is zero, that is, if

$$\theta(f, x_A) = 0, \quad (2C-3)$$

then

$$D(f, f_X) = \int_{-L/2}^{L/2} a(f, x_A) \exp(+j2\pi f_X x_A) dx_A \quad (2C-4)$$

or

$$D(f, f_X) = \int_{-L/2}^{L/2} a(f, x_A) \cos(2\pi f_X x_A) dx_A + j \int_{-L/2}^{L/2} a(f, x_A) \sin(2\pi f_X x_A) dx_A. \quad (2C-5)$$

If the amplitude response (amplitude window) $a(f, x_A)$ is an *even* function of x_A , that is, if

$$a(f, -x_A) = a(f, x_A), \quad (2C-6)$$

then the product $a(f, x_A) \cos(2\pi f_X x_A)$ is an even function of x_A , and the product $a(f, x_A) \sin(2\pi f_X x_A)$ is an odd function of x_A . Therefore, the far-field beam pattern given by (2C-5) reduces to

$$D(f, f_X) = 2 \int_0^{L/2} a(f, x_A) \cos(2\pi f_X x_A) dx_A. \quad (2C-7)$$

Equation (2C-7) is a *real, even* function of spatial frequency $f_X = u/\lambda$ and, hence, direction cosine u , since $D(f, -f_X) = D(f, f_X)$ and $D(f, -u) = D(f, u)$.

If the amplitude response (amplitude window) $a(f, x_A)$ is an *odd* function of x_A , that is, if

$$a(f, -x_A) = -a(f, x_A), \quad (2C-8)$$

then the product $a(f, x_A) \cos(2\pi f_X x_A)$ is an odd function of x_A , and the product $a(f, x_A) \sin(2\pi f_X x_A)$ is an even function of x_A . Therefore, the far-field beam pattern given by (2C-5) reduces to

$$D(f, f_X) = j 2 \int_0^{L/2} a(f, x_A) \sin(2\pi f_X x_A) dx_A. \quad (2C-9)$$

Equation (2C-9) is an *imaginary, odd* function of spatial frequency $f_X = u/\lambda$ and, hence, direction cosine u , since $D(f, -f_X) = -D(f, f_X)$ and $D(f, -u) = -D(f, u)$.

Appendix 2D Computing the Normalization Factor

The far-field beam pattern of a linear aperture lying along the X axis is given by [see (2.1-9)]

$$D(f, f_X) = \int_{-L/2}^{L/2} A(f, x_A) \exp(+j2\pi f_X x_A) dx_A , \quad (2D-1)$$

where

$$A(f, x_A) = a(f, x_A) \exp(+j\theta(f, x_A)) \quad (2D-2)$$

is the complex frequency response (complex aperture function) of the linear aperture [see (2.1-10)]. Computing the magnitude of (2D-1) yields

$$\begin{aligned} |D(f, f_X)| &= \left| \int_{-L/2}^{L/2} A(f, x_A) \exp(+j2\pi f_X x_A) dx_A \right| \\ &\leq \int_{-L/2}^{L/2} |A(f, x_A) \exp(+j2\pi f_X x_A)| dx_A \\ &\leq \int_{-L/2}^{L/2} |A(f, x_A)| |\exp(+j2\pi f_X x_A)| dx_A \\ &\leq \int_{-L/2}^{L/2} |a(f, x_A)| dx_A . \end{aligned} \quad (2D-3)$$

Therefore,

$$\max |D(f, f_X)| = \int_{-L/2}^{L/2} |a(f, x_A)| dx_A , \quad (2D-4)$$

and by following the steps in (2D-3), it can also be shown that

$$\max |\mathcal{S}(f)| = \int_{-L/2}^{L/2} |a(f, x_A)| dx_A , \quad (2D-5)$$

where $\mathcal{S}(f)$ is the element sensitivity function (see [Appendix 2A](#)). The absolute value of the real amplitude response $a(f, x_A)$ is required in (2D-4) and (2D-5) because $a(f, x_A)$ can have, in general, both positive and negative values as a function of x_A .

Equation (2D-4) is the absolute maximum value of $|D(f, f_X)|$. The actual maximum value may be less than (2D-4) as indicated by (2D-3). However, if $a(f, x_A) \geq 0$, then the normalization factor D_{\max} is

$$D_{\max} = \max |D(f, f_X)| = \int_{-L/2}^{L/2} a(f, x_A) dx_A \quad (2D-6)$$

or

$$D_{\max} = \max |S(f)| = \int_{-L/2}^{L/2} a(f, x_A) dx_A \quad (2D-7)$$

Note that if (2D-1) is evaluated at broadside (i.e., at $f_x = 0$) and if the phase response $\theta(f, x_A) = 0$, then

$$D(f, 0) = \int_{-L/2}^{L/2} a(f, x_A) dx_A \quad (2D-8)$$

and

$$|D(f, 0)| = \left| \int_{-L/2}^{L/2} a(f, x_A) dx_A \right| \leq \int_{-L/2}^{L/2} |a(f, x_A)| dx_A. \quad (2D-9)$$

If in addition $a(f, x_A) \geq 0$, then

$$|D(f, 0)| = \left| \int_{-L/2}^{L/2} a(f, x_A) dx_A \right| = \int_{-L/2}^{L/2} a(f, x_A) dx_A, \quad (2D-10)$$

and by comparing (2D-6) and (2D-10),

$$D_{\max} = \max |D(f, f_x)| = |D(f, 0)| \quad (2D-11)$$

For example, the cosine amplitude window is given by [see (2.2-30)]

$$a(f, x_A) = A_A \cos(\pi x_A / L) \text{rect}(x_A / L). \quad (2D-12)$$

Since $a(f, x_A) \geq 0$ (see Fig. 2.2-8),

$$\begin{aligned} D_{\max} &= A_A \int_{-L/2}^{L/2} \cos(\pi x_A / L) dx_A \\ &= A_A \frac{L}{\pi} \sin(\pi x_A / L) \Big|_{-L/2}^{L/2} \\ &= A_A \frac{L}{\pi} [\sin(\pi/2) - \sin(-\pi/2)] \\ &= 2A_A L / \pi. \end{aligned} \quad (2D-13)$$

Equation (2D-13) agrees with (2.2-34).